Technische Universität Graz

Sparsity optimized high order finite element functions for H(div) on simplices

S. Beuchler, V. Pillwein, S. Zaglmayr

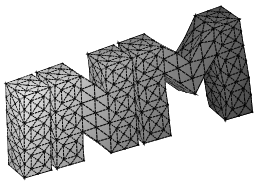

Berichte aus dem Institut für Numerische Mathematik

Bericht 2010/11

Technische Universität Graz

Sparsity optimized high order finite element functions for H(div) on simplices

S. Beuchler, V. Pillwein, S. Zaglmayr

Berichte aus dem Institut für Numerische Mathematik

Bericht 2010/11

Technische Universität Graz
Institut für Numerische Mathematik
Steyrergasse 30
A 8010 Graz

WWW: http://www.numerik.math.tu-graz.at

Sparsity optimized high order finite element functions for H(div) on simplices

Sven Beuchler*, Veronika Pillwein#, and Sabine Zaglmayr**

* Johann Radon Institute for Computational and Applied Mathematics
Austrian Academy of Sciences Altenbergerstraße 69, 4040 Linz, Austria,
sven.beuchler@ricam.oeaw.ac.at

Research Institute for Symbolic Computation
Altenberger Straße 69
A-4040 Linz, Austria
veronika.pillwein@risc.jku.at

** Institute for Computational Mathematics, Graz University of Technology,
Steyrergasse 30, 8010 Graz, Austria,
sabine.zaglmayr@tugraz.at

Abstract This paper deals with conforming high-order finite element discretizations of the vector-valued function space $H(\mathrm{div})$ in 2 and 3 dimensions. A new set of hierarchic basis functions on simplices with the following two main properties is introduced. Provided an affine simplicial triangulation, first, the divergence of the basis functions is L_2-orthogonal, and secondly, the L_2-inner product of the interior basis functions is sparse with respect to the polynomial order p. The construction relies on a tensor-product based construction with properly weighted Jacobi polynomials as well as an explicit splitting of the higher-order basis functions into solenoidal and non-solenoidal ones. The basis is suited for fast assembling strategies. The general proof of the sparsity result is done by the assistance of computer algebra software tools. Several numerical experiments document the proved sparsity patterns and practically achieved condition numbers for the parameter-dependent div-div problem. Even on curved elements a tremendous improvement in condition numbers is observed. The precomputed mass and stiffness matrix entries in general form are available online.

1 Introduction

In this paper, we investigate the space of vector-valued functions with square-integrable divergence

$$H(\mathrm{div},\Omega) := \{u \in L_2(\Omega)^d \ : \ \mathrm{div}\ u \in L_2(\Omega)\} \tag{1.1}$$

and conforming hp-finite element discretizations for open bounded Lipschitz-domains $\Omega \subset \mathbb{R}^d$ with $d = 2, 3$.

For more than twenty years, spectral methods, [20], as well as the p-version and the hp-version of the finite element method, see e.g. [15], [13], [29], [32], and the references therein, have become more and more popular. In the classical (h-version) finite element method, convergence of a piecewise polynomial discrete solution (typically of fixed low degree) to the exact solution is achieved by decreasing the mesh size h. In the p-version of the finite element method the mesh is fixed and convergence is obtained by increasing the polynomial degree p. Combing both ideas, i.e. allowing simultaneously for a mesh refinement in h as well as increasing the polynomial degree p,

yields the *hp*-version of the FEM [6]. By the proper combination of local h-refinement and local p-enrichment the *hp*-version achieves tremendously faster convergence rates with respect to the number of unknowns in case of piecewise analytic solutions even in the presence of singularities, see e.g. [29], [33].
But, a naive approach to high-order finite element methods in general suffers from dense element matrices with up to $\mathcal{O}(p^{2d})$ nonzero entries. Moreover, when using standard numerical quadrature, the calculation of each entry of the element matrix requires $\mathcal{O}(p^d)$ operations; resulting in the total cost of $\mathcal{O}(p^{3d})$ for assembling one element matrix. Hence, additionally to the question of fast and efficient solvers, also fast assembling techniques, condition numbers (with respect to p) and sparsity of the element matrices become an issue in spectral and high-order finite element methods.
The high-quadrature costs per matrix entry can be reduced by sum-factorization: using basis functions which are constructed as (warped) tensor-products the costs for assembling the element stiffness matrix can be reduced from $\mathcal{O}(p^{3d})$ to $\mathcal{O}(p^{d+1})$ in case of piecewise constant coefficients; see [25], [20] for H^1- and L_2-conforming discretizations. In view of fast assembling and fast matrix-vector multiplications one additionally heads for sparse element matrices with $\mathcal{O}(p^d)$ non-zero entries. The construction of basis functions which implies sparse element matrices for p- and *hp*-FEM on simplicial meshes is by no means trivial and depends on the smoothness properties of the underlying finite element space. The Dubiner basis, as initially proposed in [21, 17] for triangles and generalized by [31] to tetrahedra, is a hierarchical set of L_2-orthogonal polynomials on simplices. The basis can be used for discontinuous (L_2-conforming) FE discretizations and implies diagonal mass matrices for piecewise constant coefficients and affine triangulations.
Conforming finite element discretization has to satisfy the smoothness properties of the underlying function space, i.e. continuity across element-interfaces for H^1-conformity, and respectively, only normal continuity across element-interfaces to guarantee $H(\mathrm{div})$-conformity [12]. But by enforcing inter-element-continuity constraints one generally loses the L_2-orthogonality of the basis functions. For H^1-conforming discretizations at least sparsity of the element mass and stiffness matrix (for piecewise constant coefficients) can be regained. In [31], a new H^1-conforming basis for triangular and tetrahedral elements involving warped tensor-products of Legendre- and properly mixed-weighted Jacobi polynomials is introduced. Applying this basis in the discretization of diffusion-type problems with piecewise constant coefficients sparse stiffness and mass matrices are observed, see [30]. A further H^1-conforming basis on simplices with proven sparsity of the element stiffness and mass matrix, i.e. $\mathcal{O}(p^d)$ non-zero entries, is proposed in [10], [8], respectively. Compared to the basis suggested in [31], the bases in [10, 8] use increased weights of the Jacobi polynomials in certain directions. For piecewise constant coefficients and affine element transformations each nonzero entry in the global matrix can be computed in $\mathcal{O}(1)$ operations. A rigorous proof of the sparsity property for the basis of Karniadakis-Sherwin [31] followed in [9].

The function space $H(\mathbf{div})$ and conforming finite element discretizations The vector-valued function space $H(\mathrm{div})$ occurs in many applications, e.g. in electromagnetics, elasticity, fluid dynamics, as well as in dual or mixed formulations of diffusion-type problems. The analysis of $H(\mathrm{div})$-problems and their conforming discretizations are governed by the mapping properties of the divergence-operator, as clarified in many works e.g. [18, 11, 13, 14, 5]. Namely, the kernel and range of the div-operator are

$$\{v \in H(\mathrm{div}) \,:\, \mathrm{div}\, v = 0\} = \mathrm{curl}\big(H(\mathrm{curl},\Omega)\big), \qquad \text{and} \qquad \mathrm{div}\big(H(\mathrm{div},\Omega)\big) = L_2(\Omega) \tag{1.2}$$

for simply connected domains Ω with connected boundary (cf. the exactness of the de Rham Sequence [11, 18]). If Ω lacks the latter topological properties the kernel and range spaces in (1.2) have to be extended by finite dimensional cohomology spaces (see [11]). $H(\mathrm{div})$-conformity requires normal continuity towards element interfaces. For a detailed introduction to classical (h-version) $H(\mathrm{div})$-conforming finite element discretizations we refer to the pioneering works [23, 24, 27] and the textbooks [12, 18]. $H(\mathrm{div})$-conforming finite element methods suited for p- and *hp*-discretizations were heavily investigated in the last decade.
To guarantee stability and convergence of $H(\mathrm{div})$-conforming FE methods mapping properties analogue to (1.2) have to be valid also on the discrete level, see e.g. [11, 16, 5]. Approximation

results for *hp*-discretization can be obtained in the course of the de Rham diagram, as done in [14]. A first general construction strategy for hierarchical $H(\mathrm{div})$-conforming (normal continuous facet-cell-based) basis functions of arbitrary polynomial degrees on simplicial meshes was introduced by Ainsworth-Coyle in [2]. In [35], a new construction technique for $H(\mathrm{div})$-conforming basis functions based on first, a hierarchic construction using warped tensor-products of orthogonal polynomials and secondly, on an explicit splitting of the set of higher-order basis functions into divergence-free functions and non-divergence-free completion functions, is introduced. This splitting implies e.g. the (local) exactness of the de Rham sequence for arbitrary varying polynomial degrees by construction as well as parameter-robustness even for simple preconditioning techniques (see [35],[28]).

Sparsity for $H(\mathrm{div})$-conforming discretizations To the knowledge of the authors works investigating and improving the sparsity of $H(\mathrm{div})$-conforming elements as available for L_2- and H^1-conforming high-order discretizations are still an open problem in the literature. Nevertheless, the $H(\mathrm{div})$-conforming basis functions on affine quadrilaterals and hexahedra presented in [35] yield sparse element matrices with $\mathcal{O}(p^d)$ nonzero matrix entries for affine linear transformations and piecewise constant coefficients. Moreover, by using Legendre-type polynomials the divergence of the higher order basis functions are L_2-orthogonal on affine tensor product elements.
In this work we generalize this property to affine, possibly unstructured simplicial meshes. We introduce a new set of basis functions for $H(\mathrm{div})$-conforming *hp*-finite element spaces, which yields an optimal sparsity pattern for system matrices derived from the discretization of the bilinear form

$$a(u,v) := (\varepsilon\,\mathrm{div} u, \mathrm{div} v) + (\kappa\, u, v) \tag{1.3}$$

for piecewise constant parameters ε, κ and $(\cdot,\cdot)$ denoting the $L_2(\Omega)$-inner product. In fact we obtain a set of higher-order basis functions $[\psi_i]_{i=1}^N$ such that the according fluxes $\{\mathrm{div}\,\psi_i\}_{i=1}^N$ are L_2-orthogonal (provided an affine element transformation).
The construction of the basis functions rely on the construction principles suggested in [35] in combination with the ideas of [31, 17]. These construction principles can be summarized as follows:

1. As common, the basis $[\Psi^{(0)}]$ of the low-order space are chosen by the classical Raviart-Thomas elements [23] of zero-th order.
2. The set of divergence-free basis functions $[\Psi^{(1)}]$ are chosen as the curl of the hierarchic $H(\mathrm{curl})$-conforming completion functions as presented in [35]. But in this work, we rely on products of mixed-weighted Jacobi-polynomials (instead of Legendre-type polynomials), where the weights are chosen in analogy to the H^1-conforming basis suggested in [10, 8].
3. The set of cell-based basis functions $[\Psi^{(2)}]$ spanning the non-divergence-free subspace are chosen such that $[\mathrm{div}(\Psi^{(2)})]$ coincides with the Dubiner basis (modulo constants).

This construction implies L_2-orthogonality of the fluxes of the basis functions (up to the low-order shape functions). The proof of the sparsity of the mass matrix requires the assistance of a computer algebra system as done for $H^1(\Omega)$ in [8]. Despite assuming affine element transformations and piecewise constant coefficients, the reader should keep in mind that the introduced finite element basis $[\Psi^{(0)}, \Psi^{(1)}, \Psi^{(2)}]$ form a hierarchical set of $H(\mathrm{div})$-conforming basis functions and hence are applicable also in general settings on unstructured (curved) simplicial meshes. Moreover, the new finite element basis provides the same robust preconditioning properties as the basis in [35].

Applications of the bilinear form The bilinear form (1.3) arises e.g. in the dual formulations of diffusion problems as follows. For simplicity of presentation, we investigate the diffusion-reaction problem with homogenous boundary conditions:

Find $\phi \in H^1_{0,\Gamma_1}(\Omega) = \{\phi \in H^1(\Omega) \,:\, \phi = 0 \text{ on } \Gamma_1\}$, such that

$$(\varepsilon\nabla\phi, \nabla\zeta) + (\kappa\phi, \zeta) = (f, \zeta) \quad \forall \zeta \in H^1_{0,\Gamma_1}(\Omega) \tag{1.4}$$

with $\Gamma_1 \cap \Gamma_2 = \emptyset$ and $\Gamma_1 \cup \Gamma_2 = \partial\Omega$ and parameters $0 < \varepsilon, \kappa$ almost everywhere. The dual mixed formulation of this problem reads, [12]:

Find $u \in H_{0,\Gamma_2}(\mathrm{div}, \Omega) = \{v \in H(\mathrm{div}, \Omega) \,:\, v \cdot n = 0 \text{ on } \Gamma_2\}$ and $\phi \in L_2(\Omega)$ such that

$$\begin{aligned} (\varepsilon^{-1} u, v) + (\phi, \mathrm{div}\, v) &= 0 \qquad && \forall v \in H_{0,\Gamma_2}(\mathrm{div}, \Omega), \\ (\mathrm{div}\, u, \zeta) - (\kappa\phi, \zeta) &= -(f, \rho) && \forall \zeta \in L_2(\Omega), \end{aligned} \tag{1.5}$$

where n denotes the outer normal vector on $\partial\Omega$. Eliminating the primal variable ϕ yields the dual formulation:

Find $u \in H_{0,\Gamma_2}(\mathrm{div}) := \{v \in H(\mathrm{div}) \,:\, v \cdot n = 0 \text{ on } \Gamma_2\}$ such that

$$(\varepsilon\ \mathrm{div}\, u, \mathrm{div}\, v) + (\kappa\, u, v) = -(\varepsilon\, f, \mathrm{div}\, v) =: \langle F, v\rangle_\Omega \qquad \forall v \in H_{0,\Gamma_2}(\mathrm{div}) \tag{1.6}$$

involving the bilinear form (1.3).

Overview This manuscript is organized as follows. In section 2, we summarize all properties of Jacobi polynomials and their primitives which are required in the sequel. In section 3, the new set of shape functions on general affine triangles are defined. The sparsity of the element mass matrix is proven for a reference element. Section 4 includes the 3 dimensional setting, as there is the definition of shape functions on general tetrahedra and a proof of the sparsity of the element mass matrix for reference tetrahedra. Assuming affine element transformations the sparsity of the global system matrix discretizing bilinear form (1.3) is verified for piecewise constant coefficients ε and κ in section 5. Computational properties and numerical experiments are summarized in section 6.

2 Properties of Jacobi polynomials with weight $(1-x)^\alpha$

For the definition of our basis functions on the reference element, Jacobi polynomials are required. In this section, we summarize the most important properties of Jacobi polynomials. We refer the reader to the books of Abramowitz and Stegun, [1], Andrews, Askey and Roy, [3], and Tricomi, [34], for more details.
Let

$$P_n^{(\alpha,\beta)}(x) = \frac{1}{2^n n!(1-x)^\alpha(1+x)^\beta}\frac{\mathrm{d}^n}{\mathrm{d}x^n}\left((1-x)^\alpha(1+x)^\beta(x^2-1)^n\right) \quad n \in \mathbb{N}_0,\ \alpha, \beta > -1 \tag{2.1}$$

be the nth Jacobi polynomial with respect to the weight function $(1-x)^\alpha(1+x)^\beta$. The function $P_n^{(\alpha,\beta)}(x)$ is a polynomial of degree n, i.e. $P_n^{(\alpha,\beta)}(x) \in \mathbb{P}_n((-1,1))$, where $\mathbb{P}_n(I)$ is the space of all polynomials of degree n on the interval I. In the special case $\alpha = \beta = 0$, the functions $P_n^{(0,0)}(x)$ are called Legendre polynomials. Moreover, let

$$\hat{P}_n^{(\alpha,\beta)}(x) = \int_{-1}^{x} P_{n-1}^{(\alpha,\beta)}(y)\ \mathrm{d}y \quad n \geq 1, \quad \hat{P}_0^{(\alpha,\beta)}(x) = 1 \tag{2.2}$$

be the nth integrated Jacobi polynomial.
We would like to mention that the integrated Jacobi polynomial (2.2) can be expressed as Jacobi polynomial (2.1) with modified weights, i.e.

$$\hat{P}_n^{(\alpha,\beta)}(x) = \frac{2}{n+\alpha+\beta-1}\left[P_n^{(\alpha-1,\beta-1)}(x) - P_n^{(\alpha-1,\beta-1)}(-1)\right], \tag{2.3}$$

for $\alpha > 0$ or $\beta > 0$. This is easy to be seen, since the derivatives of Jacobi polynomials are again Jacobi polynomials with shifted parameters, i.e.

$$\frac{\mathrm{d}}{\mathrm{d}x}P_n^{(\alpha,\beta)}(x) = \frac{n+\alpha+\beta+1}{2}P_{n-1}^{(\alpha+1,\beta+1)}(x),$$

see [3].
In the following, we use only the Jacobi and integrated Jacobi polynomials with weight $(1-x)^\alpha$, i.e. $\beta = 0$. Therefore, we omit the second index β in (2.1), (2.2) and use the notation $P_n^{(\alpha,0)}(x) = p_n^\alpha(x)$ and $\hat{P}_n^{(\alpha,0)}(x) = \hat{p}_n^\alpha(x)$, respectively. In this case, relation (2.3) simplifies to

$$\hat{p}_n^\alpha(x) = \frac{2}{n+\alpha-1} P_n^{(\alpha-1,-1)}(x).$$

There are several relations between the Jacobi polynomials (2.1) and the integrated Jacobi polynomials (2.2) which only hold in the special case of $\beta = 0$ in (2.1), (2.2). These relations have been proved in [10], [8] and [9]. In the present paper the main relations required for proving the orthogonality of our basis function in $H(\mathrm{div})$ are

$$\int_{-1}^{1} (1-x)^\alpha p_j^\alpha(x) p_l^\alpha(x)\, \mathrm{d}x = \rho_j^\alpha \delta_{jl}, \quad \text{where } \rho_j^\alpha = \frac{2^{\alpha+1}}{2j+\alpha+1}, \tag{2.4}$$

$$(\alpha-1)\hat{p}_j^\alpha(y) = (1-y)p_{j-1}^\alpha(y) + 2p_j^{\alpha-2}(y), \quad \alpha > 1, j \geq 1. \tag{2.5}$$

For the proof of the sparsity of the mass matrix we will need additional relations which are proven in [10, 8, 9] and summarized in the appendix A. Jacobi- and integrated Jacobi-type polynomials can be evaluated efficiently by three term recurrences as summarized in the appendix.

3 The element stiffness matrix on triangles

In this section we define the shape functions on a general triangle, which are appropriate for $H(\mathrm{div})$-conforming (i.e. normal continuous) discretizations and imply sparse element stiffness and mass matrices. In view of varying polynomial order and normal continuity of the basis functions we rely on the common edge-cell-based construction, see e.g. [13, 2]. Hence, in general, the polynomial degree can vary on each edge and the interior (cell) of the element. Nevertheless, for ease of notation we assume a uniform polynomial order denoted by the parameter p, since the generalization to varying polynomial degrees should be obvious.

3.1 Definition of $H(\mathrm{div})$-conforming shape functions on 2d simplices

Let Δ denote an arbitrary non-degenerated simplex $\Delta \subset \mathbb{R}^2$ defined as the convex hull of the three vertices $\mathcal{V} = \{V_1, V_2, V_3\}$ with $V_i \in \mathbb{R}^2$, and $\lambda_1, \lambda_2, \lambda_3 \in P^1(\Delta)$ its barycentric coordinates which are uniquely defined by $\lambda_i(V_j) = \delta_{ij}$. For functions $v : \mathbb{R}^2 \to \mathbb{R}$ we define the vector-valued curl-operator $\mathrm{Curl}(v) = \left(\frac{\partial v}{\partial y}, -\frac{\partial v}{\partial x}\right)^\top$. Following [35], we construct the following hierarchical set of shape functions on the triangle Δ using an explicit edge-cell-based basis of the higher-order divergence-free functions and a cell-based basis for the higher-order non-divergence-free completion functions.

Edge-based shape functions For each edge $[e_1, e_2]$, running from vertex V_{e_1} to V_{e_2}, we define the Raviart-Thomas function of order zero, [23, 11], in barycentric coordinates as

$$\psi_0^{[e_1,e_2]} := \mathrm{Curl}(\lambda_{e_1})\, \lambda_{e_2} - \lambda_{e_1}\, \mathrm{Curl}(\lambda_{e_2}). \tag{3.1}$$

The higher-order edge-based shape functions are defined as the vector curl of appropriate edge based scalar fields, namely

$$\psi_i^{[e_1,e_2]} := \mathrm{Curl}\left(\hat{p}_i^0\left(\tfrac{\lambda_{e_2}-\lambda_{e_1}}{\lambda_{e_1}+\lambda_{e_2}}\right)(\lambda_{e_1}+\lambda_{e_2})^i\right), \quad \text{for } 2 \leq i \leq p+1. \tag{3.2}$$

Let $[\Psi_0] := \left[\psi_0^{[1,2]}, \psi_0^{[2,3]}, \psi_0^{[3,1]}\right]$ denote the set of low-order basis functions and $[\Psi^{[e_1,e_2]}] := \left[\psi_i^{[e_1,e_2]}\right]_{i=2}^p$ be the row vector of the higher-order edge based basis functions of one fixed edge,

and

$$[\Psi_E] := \left[\begin{array}{ccc} [\Psi^{[1,2]}] & [\Psi^{[2,3]}] & [\Psi^{[3,1]}] \end{array} \right] \tag{3.3}$$

denote the row vector of all higher-order edge-based basis functions. The edge-based functions (3.3) are chosen such that their normal trace span $P^p([V_\alpha, V_\beta])$ on the associated edge, the one running from V_α to V_β, while identically vanishing on all other edges.

Interior (cell-based) shape functions The cell-based basis functions are constructed in two types. First, we define the divergence-free shape functions

$$\psi_{ij}^{(1)}(x,y) := \operatorname{Curl}\left(u_i(x,y)\; v_{ij}(x,y)\right) \qquad \text{for } i \geq 2, j \geq 1, i+j \leq p+1 \tag{3.4}$$

and complete the basis by the non-divergence-free interior shape functions

$$\psi_{1j}^{(2)}(x,y) := 2\psi_0^{[1,2]}(x,y)\, \hat{p}_j^3(2\lambda_3 - 1) \qquad \text{for } 1 \leq j \leq p-1, \tag{3.5}$$

$$\psi_{ij}^{(2)}(x,y) := (\operatorname{Curl} u_i(x,y))\; v_{ij}(x,y) \qquad \text{for } i \geq 2,\; j \geq 1, i+j \leq p+1, \tag{3.6}$$

where $\psi_0^{[1,2]}(x,y)$ denotes the Raviart-Thomas function (3.1). In addition, the auxiliary functions u_i and v_{ij} are chosen by

$$u_i(x,y) := \hat{p}_i^0\left(\tfrac{\lambda_2-\lambda_1}{\lambda_1+\lambda_2}\right)(\lambda_1+\lambda_2)^i \quad \text{and} \quad v_{ij}(x,y) := \hat{p}_j^{2i-1}(2\lambda_3-1), \tag{3.7}$$

respectively, where the baryzentrical coordinates depend on x and y. Note that these are the polynomials used in the definition of the H^1-cell based basis functions $\phi_{ij}^C = u_i v_{ij}$ in [10] and [9] for $a = 1$, respectively. The set of all interior basis functions is denoted by

$$[\Psi_I] := \left[\begin{array}{cc} [\Psi_1] & [\Psi_2] \end{array} \right] \quad \text{with} \quad [\Psi_1] = \left[\psi_{ij}^{(1)}\right]_{i\geq 2, j\geq 1}^{i+j\leq p+1} \quad \text{and} \quad [\Psi_2] := \left[\psi_{ij}^{(2)}\right]_{i=1,j=1}^{p,\min\{p+1-i,p-1\}}. \tag{3.8}$$

The cell-based functions (3.8) have vanishing normal trace on all edges.
Finally, the row vector of all basis functions is denoted by

$$[\Psi] := \left[\begin{array}{ccc} [\Psi_0] & [\Psi_E] & [\Psi_I] \end{array} \right]. \tag{3.9}$$

Lemma 3.1. *The shape functions* $[\Psi]$*, see* (3.9)*, are linearly independent spanning* $(P^p(\Delta))^2$ *and* $div([\Psi_2])$ *spanning* $P^{p-1}(\Delta)|_{\mathbb{R}}$*.*

Proof. The result follows from the fact that the proofs presented in [35] also hold for the suggested auxiliary functions (3.7). □

Remark 3.2. $[\Psi]$ *is a basis for the Raviart-Thomas spaces of second kind as introduced in [24]. Decreasing the polynomial degrees for the divergence-free functions by one yields FE-space with the same approximation properties as Raviart-Thomas spaces of the first family [23].*

3.2 Properties of the basis functions and orthogonality relations

To simplify the presentation, we prove the orthogonality properties of the suggested shape functions for a (fixed) reference triangle. The generalization to an arbitrary two-dimensional simplex then follows by the Piola transformation (see chapter 5). Let $\hat{\triangle}$ be the reference triangle with the vertices $(-1,-1)$, $(1,-1)$ and $(0,1)$ as depicted in Figure 1. In this case, the corresponding baryzentrical coordinates are

$$\lambda_1(x,y) = \frac{1-2x-y}{4}, \qquad \lambda_2(x,y) = \frac{1+2x-y}{4}, \qquad \lambda_3(x,y) = \frac{1+y}{2}$$

and the auxiliary functions (3.7) for the cell-based shape functions equal

$$u_i(x,y) = \hat{p}_i^0\left(\frac{2x}{1-y}\right)\left(\frac{1-y}{2}\right)^i, \qquad v_{ij}(x,y) = v_{ij}(y) = \hat{p}_j^{2i-1}(y). \tag{3.10}$$

The next lemma summarizes the divergence of the basis functions (3.1), (3.2), (3.4)-(3.6).

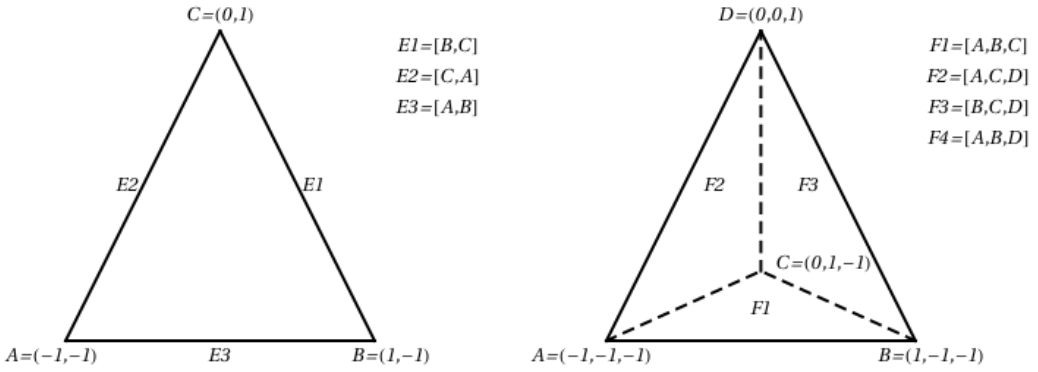

Figure 1: Notation of the vertices and edges/faces on the reference element $\hat{\triangle}$ for 2d and 3d.

Lemma 3.3. *Let* $[\Psi_0]$, $[\Psi_E]$ *and* $[\Psi_I]$ *be defined by* (3.1), (3.3), (3.8), *respectively. Then, the relations*

$$\begin{aligned} [\nabla \cdot \Psi_0] &= -\tfrac{1}{2}\mathbf{1}, \quad [\nabla \cdot \Psi_E] = \mathbf{0}, \quad [\nabla \cdot \Psi_1] = \mathbf{0}, && (3.11)\\ \nabla \cdot \psi_{1j}^{(2)}(x,y) &= -p_j^1(y), j \geq 1, && (3.12)\\ \nabla \cdot \psi_{ij}^{(2)}(x,y) &= -p_{i-1}^0\left(\frac{2x}{1-y}\right)\left(\frac{1-y}{2}\right)^{i-1} p_{j-1}^{2i-1}(y), \quad i \geq 2, j \geq 1 && (3.13) \end{aligned}$$

hold.

Proof. The first identity in (3.11) is easily calculated, the two other ones are direct consequences of $\nabla \cdot (\text{Curl}) \equiv 0$. Because of this and since $v_{ij}(y)$ depends only on y, we also immediately obtain (3.13), i.e.

$$\begin{aligned} \nabla \cdot \psi_{ij}^{(2)}(x,y) &= -\frac{\partial u_i}{\partial x}(x,y)\frac{\partial v_{ij}}{\partial y}(x,y) \\ &= -p_{i-1}^0\left(\frac{2x}{1-y}\right)\left(\frac{1-y}{2}\right)^{i-1} p_{j-1}^{2i-1}(y). \end{aligned}$$

The last identity (3.12) is proved in a similar way. On $\hat{\triangle}$, there holds $\psi_0^{[1,2]}(x,y) = \frac{1}{4}\begin{bmatrix} -x \\ 1-y \end{bmatrix}$. This yields

$$\begin{aligned} \nabla \cdot \psi_{1j}^{(2)}(x,y) &= 2\nabla \cdot \psi_0^{[1,2]}(x,y)\,\hat{p}_j^3(y) + 2\psi_0^{[1,2]}(x,y) \cdot \nabla \hat{p}_j^3(y) \\ &= \frac{1-y}{2} p_{j-1}^3(y) - \hat{p}_j^3(y) = -p_j^1(y). \end{aligned}$$

Note that we have used relation (2.5) with $\alpha = 3$ in the last step. This proves the assertion. □

Remark 3.4. *The special choice* (3.10) *of the auxiliary functions implies that the divergence of the non-divergence-free interior shape functions* (3.13), (3.12) *coincides with the shape functions suggested by Dubiner [17] for the* L_2*-conforming triangle.*

Remark 3.5. *Since* $p_0^0(z) = 1$, *relation* (3.12) *can be viewed as a special case of* (3.13) *with* $i = 1$.

The orthogonality of the interior basis functions (3.4)-(3.6) with respect to the $H(\text{div})$-seminorm is now immediate.

Theorem 3.6. *Let* $[\Psi]$ *be defined by* (3.9)*. Then, the fluxes* $[\nabla\cdot\Psi_I]$ *are* L_2*-orthogonal to* $[\nabla\cdot\Psi]$*. More precisely, the only nonzero div-div inner-products of the basis* $[\Psi]$ *are*

$$\begin{aligned}(\nabla\cdot\psi_{ij}^{(2)},\nabla\cdot\psi_{kl}^{(2)})_{0,\hat{\triangle}} &= \frac{2\delta_{i,k}\delta_{j,l}}{(2i-1)(i+j-1)}, && i\geq 1, j\geq 1,\\ (\nabla\cdot\psi_0^{E_m},\nabla\cdot\psi_0^{E_n})_{0,\hat{\triangle}} &= \tfrac{1}{2}, && m,n\in\{1,2,3\}.\end{aligned}$$

Proof. The result for $(\nabla\cdot\psi_0^{E_m},\nabla\cdot\psi_0^{E_n})_{0,\hat{\triangle}}$ follows by straightforward computation. Performing the Duffy transformation to the non-divergence-free basis functions (3.6), taking the results of Lemma 3.3 and exploiting the orthogonality relations (2.4) of Jacobi polynomials one obtains

$$\begin{aligned}\int_{\hat{\triangle}}\nabla\cdot\psi_{ij}^{(2)}\,\nabla\cdot\psi_{kl}^{(2)}\,\mathrm{d}(x,y) &= \int_{-1}^{1}p_{i-1}^{0}(\xi)\,p_{k-1}^{0}(\xi)\,\mathrm{d}\xi\int_{-1}^{1}\left(\frac{1-y}{2}\right)^{i+k-1}p_{j-1}^{2i-1}(y)\,p_{l-1}^{2k-1}(y)\,\mathrm{d}y\\ &= \frac{2\delta_{i,k}}{(2i-1)}\int_{-1}^{1}\left(\frac{1-y}{2}\right)^{2i-1}p_{j-1}^{2i-1}(y)\,p_{l-1}^{2i-1}(y)\,\mathrm{d}y\\ &= \frac{2\delta_{i,k}\delta_{j,l}}{(2i-1)(i+j-1)}.\end{aligned}$$

Testing with the constant low-order contributions $\nabla\cdot\psi_0^{[\alpha,\beta]}=1/|\hat{\triangle}|$ yields

$$\int_{\hat{T}}\nabla\cdot\psi_0^{[\alpha,\beta]}\,\nabla\cdot\psi_{kl}^{(2)}\,\mathrm{d}(x,y)=0\qquad\text{for } k,l\geq 1.$$

Since all other shape functions are divergence-free, this proves the theorem. □

Remark 3.7. *Obviously, the interior basis functions become orthonormal with respect to the* $H(div)$*-seminorm simply by accounting the correct scaling in the definition of the auxiliary functions* (3.10)*.*

Hence, the element stiffness matrix for $[\Psi]=\left[\begin{array}{cccc}[\Psi_0] & [\Psi_E] & [\Psi_1] & [\Psi_2]\end{array}\right]$

$$\widehat{A}:=\left[\int_{\hat{\triangle}}[\nabla\cdot\Psi]^{\top}[\nabla\cdot\Psi]\,\mathrm{d}(x,y)\right]=\mathrm{diag}[\widehat{A}_{0,0},\mathbf{0},\mathbf{0},\widehat{A}_{2,2}^{I}]\tag{3.14}$$

is block diagonal with a dense 3×3 low-order block $\widehat{A}_{0,0}:=[([\nabla\cdot\Psi_0],[\nabla\cdot\Psi_0])_{0,\hat{\triangle}}]$ and a $p(p+1)/2$-dimensional diagonal matrix $\widehat{A}_{2,2}^{I}=[([\nabla\cdot\Psi_2],[\nabla\cdot\Psi_2])_{0,\hat{\triangle}}]$.
Next, we investigate the orthogonality relations of the interior shape functions with respect to the $L_2(\hat{\triangle})$-inner-product. Let

$$\widehat{M}_{II}:=\left[\int_{\hat{\triangle}}[\Psi_I]^{\top}[\Psi_I]\,\mathrm{d}(x,y)\right]\tag{3.15}$$

be the mass matrix with respect to the interior basis function on the reference element.

Lemma 3.8. *Let* $\widehat{M}_{II}$ *be defined by* (3.15)*. Then, the number of nonzero entries in* $\widehat{M}_{II}$ *per row is bounded by a constant independent of the polynomial degree. More precisely, the following orthogonality results hold:*

1. *if* $|i-k|\notin\{0,2\}$ *or* $|i-k+j-l|>2$ *then* $\left(\psi_{ij}^{(1)},\psi_{kl}^{(1)}\right)_{0,\hat{\triangle}}=0$,
2. *if* $i\neq k$ *or* $|j-l|>2$ *then* $\left(\psi_{ij}^{(2)},\psi_{kl}^{(2)}\right)_{0,\hat{\triangle}}=0$,
3. *if* $|j-l|>2$ *then* $\left(\psi_{1j}^{(2)},\psi_{1l}^{(2)}\right)_{0,\hat{\triangle}}=0$,
4. *if* $i-k\notin\{-2,0\}$ *or* $|i-k+j-l|>2$ *then* $\left(\psi_{ij}^{(1)},\psi_{kl}^{(2)}\right)_{0,\hat{\triangle}}=0$,

5. *if* $i \neq 3$ *or* $|j-l-1|>2$ *then* $\left(\psi_{ij}^{(1)},\psi_{1l}^{(2)}\right)_{0,\hat{\triangle}}=0$ *and* $\left(\psi_{ij}^{(2)},\psi_{1l}^{(2)}\right)_{0,\hat{\triangle}}=0$.

Proof. This sparsity result has been obtained by evaluating the entries of the mass matrix on the reference triangle symbolically using the algorithm developed in [8]. Carrying out such computations manually, as done e.g. for the scalar H^1-conforming triangle in [10], is very paper and time consuming. Hence, we present explicit computations only for some illustrative examples, while the general proof was carried out symbolically.
Using the three term recurrence for Jacobi polynomials (A.6) and the identity (A.4) relating integrated Jacobi and Jacobi polynomials, the basis functions $\psi_{ij}^{(1)}(x,y)$ can be rewritten as

$$\psi_{ij}^{(1)}(x,y)=\begin{pmatrix} \frac{1}{2}p_{i-2}^0\left(\frac{2x}{1-y}\right)\left(\frac{1-y}{2}\right)^{i-1}\hat{p}_j^{2i-1}(y)+\hat{p}_i^0\left(\frac{2x}{1-y}\right)p_{j-1}^{2i-1}(y) \\ -p_{i-1}^0\left(\frac{2x}{1-y}\right)\left(\frac{1-y}{2}\right)^{i-1}\hat{p}_j^{2i-1} \end{pmatrix}$$

in complete analogy to the proof of Lemma 5.1 in [10]. Also the sparsity pattern for $\left(\psi_{ij}^{(1)},\psi_{kl}^{(1)}\right)_{0,\hat{\triangle}}$ is equivalent to their result for the interior block of the stiffness matrix.
By means of the same rewriting using (A.6) and (A.4) the basis functions $\psi_{ij}^{(2)}(x,y)$ can be expressed in the simpler form

$$\psi_{ij}^{(2)}(x,y)=\begin{pmatrix} \frac{1}{2}p_{i-2}^0\left(\frac{2x}{1-y}\right) \\ -p_{i-1}^0\left(\frac{2x}{1-y}\right) \end{pmatrix}\left(\frac{1-y}{2}\right)^{i-1}\hat{p}_j^{2i-1}(y).$$

Performing the Duffy substitution the integrands decouple to

$$\begin{aligned}\left(\psi_{ij}^{(2)},\psi_{kl}^{(2)}\right)_{0,\hat{\triangle}} &= \int_{-1}^{1}\left(\tfrac{1}{4}p_{i-2}^0(\xi)p_{k-2}^0(\xi)+p_{i-1}^0(\xi)p_{k-1}^0(\xi)\right)\,\mathrm{d}\xi \\ &\quad *\int_{-1}^{1}\left(\frac{1-y}{2}\right)^{i+k-1}\hat{p}_j^{2i-1}(y)\hat{p}_l^{2k-1}(y)\,\mathrm{d}y.\end{aligned}$$

By means of the orthogonality relation (2.4), the first integral is easily evaluated and we obtain

$$\left(\psi_{ij}^{(2)},\psi_{kl}^{(2)}\right)_{0,\hat{\triangle}}=\frac{(10i-13)\delta_{i,k}}{2(2i-3)(2i-1)}\int_{-1}^{1}\left(\frac{1-y}{2}\right)^{2i-1}\hat{p}_j^{2i-1}(y)\hat{p}_l^{2i-1}(y)\,\mathrm{d}y.$$

Rewriting integrated Jacobi polynomials $\hat{p}_n^\alpha(z)$ in terms of Jacobi polynomials $p_n^\alpha(z)$ using (A.6) explains the extra two shifts in the dependence of j and l and allows to evaluate the integral using only (2.4). The final result for this part of the interior block is

$$\begin{aligned}\frac{1}{10i-13}\left(\psi_{ij}^{(2)},\psi_{kl}^{(2)}\right)_{0,\hat{\triangle}} &= -\frac{(j+1)(2i+j-1)\delta_{i,k}\delta_{j,l-2}}{(i-3/2)_2(2i+2j-2)_5}+\frac{4\delta_{i,k}\delta_{j,l-1}}{(2i+2j-3)_5}+\frac{4\delta_{i,k}\delta_{j,l+1}}{(2i+2j-5)_5} \\ &\quad +\frac{2(4i^2+2ij-8i+j^2-2j+3)\delta_{i,k}\delta_{j,l}}{(i-3/2)_2(2i+2j-4)_5}-\frac{(j-1)(2i+j-3)\delta_{i,k}\delta_{j,l+2}}{(i-3/2)_2(2i+2j-6)_5},\end{aligned}$$

where $(a)_n := a(a+1)\cdots(a+n-1)$ denotes the Pochhammer symbol.
Finally, we consider the integrals involving $\psi_{1j}^{(2)}(x,y)=\frac{1}{2}\begin{pmatrix}-x\\1-y\end{pmatrix}\hat{p}_j^3(y)$. After performing the Duffy substitution we have

$$\left(\psi_{1j}^{(2)},\psi_{1l}^{(2)}\right)_{0,\hat{\triangle}}=\int_{-1}^{1}\frac{\xi^2+4}{4}\,\mathrm{d}\xi\int_{-1}^{1}\left(\frac{1-y}{2}\right)^3\hat{p}_j^3(y)\hat{p}_l^3(y)\,\mathrm{d}y,$$

which yields the nonzero pattern as stated above. For the computation of the mixed products $\left(\psi_{ij}^{(a)},\psi_{1l}^{(2)}\right)_{0,\hat{\triangle}}$, $a=1,2$, observe that after performing the Duffy substitution we have, e.g.,

$$\left(\psi_{ij}^{(2)},\psi_{1l}^{(2)}\right)_{0,\hat{\triangle}}=\frac{1}{4}\left(\int_{-1}^{1}4p_{i-1}^0(\xi)\,\mathrm{d}\xi-\int_{-1}^{1}\xi p_{i-2}^0(\xi)\,\mathrm{d}\xi\right)\int_{-1}^{1}\left(\frac{1-y}{2}\right)^{i+1}\hat{p}_j^{2i-1}(y)\hat{p}_l^3(y)\,\mathrm{d}y.$$

The first integral w.r.t ξ is nonzero only for $i = 1$, which is excluded since $i \geq 2$. The second integral does not vanish only for $i = 3$. This together with an analogous evaluation as above yields the result. □

4 The element stiffness matrix on tetrahedra

In this section we first define the shape functions on a general 3-dimensional simplex $\triangle$, which are appropriate for normal continuous discretizations and imply sparse element stiffness and mass matrices. In order to allow for globally varying polynomial degree we use as common a face-cell-based construction [2, 13] of the basis functions. Again, for ease of notation, we assume a uniform polynomial order p.

4.1 Definition of $H(\mathbf{div})$-conforming shape functions on 3d simplices

Let Δ denote an arbitrary non-degenerated simplex $\Delta \subset \mathbb{R}^3$, its set of four vertices by $\mathcal{V} = \{V_1, V_2, V_3, V_4\}$, $V_i \in \mathbb{R}^3$, and $\lambda_1, \lambda_2, \lambda_3, \lambda_4 \in P^1(\Delta)$ its barycentric coordinates uniquely defined by $\lambda_i(V_j) = \delta_{ij}$. Again the general construction concept follows [35]: The set of face-based shape functions consists of low-order Raviart-Thomas shape functions and divergence-free shape functions. The set of interior based shape functions are split into a set of divergence-free and a set of non-divergence-free completion functions. In view of special orthogonality relations we adopt the polynomial building blocks in the tensor-product based construction by introducing properly weighted Jacobi-type polynomials in this work.

Face-based shape functions For each face $f = [f_1, f_2, f_3]$, characterized by the vertices V_{f_1}, V_{f_2} and V_{f_3}, we choose the classical Raviart-Thomas function of order zero [23] and divergence free higher-order face based basis functions as

$$\begin{aligned}
\psi_0^F &= \psi_0^{[f_1,f_2,f_3]} := \lambda_{f_1}\nabla\lambda_{f_2} \times \nabla\lambda_{f_3} + \lambda_{f_2}\nabla\lambda_{f_3} \times \nabla\lambda_{f_1} + \lambda_{f_3}\nabla\lambda_{f_1} \times \nabla\lambda_{f_2}, \\
\psi_{1j}^F &:= \nabla \times \left(\varphi_0^{[f_1,f_2]} v_{1j}^F\right), && 1 \leq j \leq p, \\
\psi_{ij}^F &:= \nabla \times \left(\nabla u_i^F v_{ij}^F\right) = -\nabla u_i^F \times \nabla v_{ij}^F, && 2 \leq i; 1 \leq j; i + j \leq p + 1
\end{aligned} \tag{4.1}$$

using the face-based Jacobi-type polynomials

$$u_i^F := \hat{p}_i^0\left(\frac{\lambda_{f_2} - \lambda_{f_1}}{\lambda_{f_2} + \lambda_{f_1}}\right)\left(\lambda_{f_2} + \lambda_{f_1}\right)^i, \qquad v_{ij}^F := \hat{p}_j^{2i-1}\left(\lambda_{f_3} - \lambda_{f_2} - \lambda_{f_1}\right), \tag{4.2}$$

and the lowest-order Nédélec function [23] corresponding to the edge $[f_1, f_2]$

$$\varphi_0^{[f_1,f_2]} := \nabla\lambda_{f_1}\,\lambda_{f_2} - \lambda_{f_1}\nabla\lambda_{f_2}. \tag{4.3}$$

Let $[\Psi_0] := \left[\psi_0^{F_1}, \psi_0^{F_1}, \psi_0^{F_1}, \psi_0^{F_1}\right]$ denote the row vector of low-order shape functions and $[\Psi^f] := \left[\left[\psi_{1j}^F\right]_{j=1}^p, \left[\psi_{ij}^F\right]_{i=2,j=1}^{i+j\leq p+1}\right]$ denote the row vector of the faced-based shape functions of one fixed face f, and

$$[\Psi_F] := \left[\begin{array}{cccc} [\Psi^{F1}] & [\Psi^{F2}] & [\Psi^{F3}] & [\Psi^{F4}] \end{array}\right] \tag{4.4}$$

be the row vector of all face-based shape functions.

Interior (cell-based) shape functions The cell-based basis functions are constructed in two types. First we define the divergence-free shape functions by the rotations

$$\begin{aligned}
\psi^{(a)}_{1jk}(x,y,z) &:= \nabla \times \big(\varphi^{[1,2]}_0(x,y,z)\, v_{2j}(x,y,z)\, w_{2jk}(x,y,z)\big), && j,k \geq 1;\ j+k \leq p,\\
\psi^{(b)}_{ijk}(x,y,z) &:= \nabla \times \big(\nabla u_i(x,y,z)\, v_{ij}(x,y,z)\, w_{ijk}(x,y,z)\big), && i \geq 2; j,k \geq 1;\ i+j+k \leq p+2,\\
\psi^{(c)}_{ijk}(x,y,z) &:= \nabla \times \big(\nabla (u_i(x,y,z)\, v_{ij}(x,y,z))\, w_{ijk}(x,y,z)\big), && i \geq 2; j,k \geq 1;\ i+j+k \leq p+2,
\end{aligned} \tag{4.5}$$

and complete the basis with the non-divergence free cell-based shape functions

$$\begin{aligned}
\widetilde{\psi}^{(a)}_{10k}(x,y,z) &:= 4\psi^{[1,2,3]}_0(x,y,z)\, w_{21k}(x,y,z), && 1 \leq k \leq p-1,\\
\widetilde{\psi}^{(b)}_{1jk}(x,y,z) &:= 2\varphi^{[1,2]}_0(x,y,z)\ \times\ \nabla w_{2jk}(x,y,z)\, v_{2j}(x,y,z), && j,k \geq 1;\ j+k \leq p,\\
\widetilde{\psi}^{(c)}_{ijk}(x,y,z) &:= w_{ijk}(x,y,z)\, \nabla u_i(x,y,z)\ \times\ \nabla v_{ij}(x,y,z), && i \geq 2; j,k \geq 1;\ i+j+k \leq p+2,
\end{aligned} \tag{4.6}$$

where $\psi^{[1,2,3]}_0(x,y,z)$ denotes the Raviart-Thomas function (4.1) associated to the bottom face $[1,2,3]$ and $\varphi^{[1,2]}_0$ is the Nédélec function (4.3) associated to the edge $[1,2]$. Furthermore, we introduce the auxiliary functions u_i, v_{ij} and w_{ijk} by the following mixed-weighted Jacobi-type polynomials

$$\begin{aligned}
u_i(x,y,z) &:= \hat{p}^0_i\left(\frac{\lambda_2-\lambda_1}{\lambda_2+\lambda_1}\right)(\lambda_2+\lambda_1)^i,\\
v_{ij}(x,y,z) &:= \hat{p}^{2i-1}_j\left(\frac{2\lambda_3-(1-\lambda_4)}{1-\lambda_4}\right)(1-\lambda_4)^j,\\
\text{and}\quad w_{ijk}(x,y,z) &:= \hat{p}^{2i+2j-2}_k(2\lambda_4-1),
\end{aligned} \tag{4.7}$$

where the baryzentrical coordinates depend on x, y and z. Finally, we denote the row vectors of the corresponding basis functions as $[\Psi_a] = \left[\psi^{(a)}_{1jk}(x,y,z)\right]^{j+k\leq p}_{j,k,\geq 1}$, $[\Psi_b] = \left[\psi^{(b)}_{ijk}(x,y,z)\right]^{i+j+k\leq p+2}_{i\geq 2,j,k,\geq 1}$, $[\Psi_c] = \left[\psi^{(c)}_{ijk}(x,y,z)\right]^{i+j+k\leq p+2}_{i\geq 2,j,k,\geq 1}$, and $[\widetilde{\Psi}_a] = \left[\widetilde{\psi}^{(a)}_{10k}(z)\right]^{p-1}_{k=1}$, $[\widetilde{\Psi}_b] = \left[\widetilde{\psi}^{(b)}_{1jk}(x,y,z)\right]^{j+k\leq p}_{j,k,\geq 1}$ and $[\widetilde{\Psi}_c] = \left[\widetilde{\psi}^{(c)}_{ijk}(x,y,z)\right]^{i+j+k\leq p+2}_{i\geq 2,j,k,\geq 1}$. The set of the interior shape functions is denoted by

$$[\Psi_I] := \begin{bmatrix} [\Psi_1] & [\Psi_2] \end{bmatrix} \quad \text{with} \quad [\Psi_1] := \begin{bmatrix} [\Psi_a] & [\Psi_b] & [\Psi_c] \end{bmatrix}, \quad [\Psi_2] := \begin{bmatrix} [\widetilde{\Psi}_a] & [\widetilde{\Psi}_b] & [\widetilde{\Psi}_c] \end{bmatrix}. \tag{4.8}$$

The complete set of low-order-face-cell-based shape functions on the tetrahedron is written as

$$[\Psi] := \begin{bmatrix} [\Psi_0] & [\Psi_F] & [\Psi_I] \end{bmatrix}. \tag{4.9}$$

Lemma 4.1. *The shape functions* $[\Psi]$ *are linearly independent spanning* $(P^p(\Delta))^3$*. Moreover, the flux* $[\nabla\cdot\Psi_2]$ *spans* $P^{p-1}(\Delta)|_{\mathbb{R}}$*, while* $[\nabla\cdot\Psi_0]$ *spans* $\mathbb{R}$*.*

Proof. The proofs of [35] also hold for the auxiliary functions (4.7), which implies the result. □

4.2 Properties of the basis functions and orthogonality relations

For a graspable presentation we prove the orthogonality properties of the suggested shape functions for a (fixed) reference tetrahedron. The general result then follows by Piola transformation (see Chapter 5). Let $\hat{\triangle}$ be the reference tetrahedron with the vertices A, B, C, and D, and the faces $F1, \ldots, F4$ as depicted in Figure 1. The baryzentrical coordinates of the chosen reference tetrahedron $\hat{\triangle}$ are

$$\lambda_1(x,y,z) = \tfrac{1-4x-2y-z}{8}, \quad \lambda_2(x,y,z) = \tfrac{1+4x-2y-z}{8}, \quad \lambda_3(y,z) = \tfrac{1+2y-z}{4}, \quad \lambda_4(z) = \tfrac{1+z}{2}. \tag{4.10}$$

Hence the Jacobi-type auxiliary functions (4.7) for the cell-based shape functions equal

$$\begin{aligned} u_i(x,y,z) &:= \hat{p}_i^0\left(\frac{4x}{1-2y-z}\right)\left(\frac{1-2y-z}{4}\right)^i, \\ v_{ij}(y,z) &:= \hat{p}_j^{2i-1}\left(\frac{2y}{1-z}\right)\left(\frac{1-z}{2}\right)^j, \\ w_{ijk}(z) &:= \hat{p}_k^{2i+2j-2}(z). \end{aligned} \tag{4.11}$$

The divergence of the basis function on the reference tetrahedron $\hat{\triangle}$ then are as follows.

Lemma 4.2. *Let* $[\Psi]$ *as defined in* (4.9) *be the basis of the local shape functions on the reference element* $\triangle := \hat{\triangle}$*. Then, the flux of the divergence-free set of basis functions vanishes, namely*

$$[\nabla \cdot \Psi_F] \equiv \mathbf{0}, \text{ and } [\nabla \cdot \Psi_1] \equiv \mathbf{0}, \tag{4.12}$$

while the flux of the remaining functions evaluate to

$$[\nabla \cdot \Psi_0] = -\frac{3}{8}\mathbf{1}, \tag{4.13}$$

$$\nabla \cdot \widetilde{\psi}_{10k}^{(a)}(x,y,z) = -p_k^2(z), \quad \forall k \geq 1, \tag{4.14}$$

$$\nabla \cdot \widetilde{\psi}_{1jk}^{(b)}(x,y,z) = -p_j^1\left(\frac{2y}{1-z}\right)\left(\frac{1-z}{2}\right)^j p_{k-1}^{2j+2}(z), \quad \forall j,k \geq 1, \tag{4.15}$$

$$\begin{aligned} \nabla \cdot \widetilde{\psi}_{ijk}^{(c)}(x,y,z) &= p_{i-1}^0\left(\frac{4x}{1-2y-z}\right)\left(\frac{1-2y-z}{4}\right)^{i-1} \\ &\quad * p_{j-1}^{2i-1}\left(\frac{2y}{1-z}\right)\left(\frac{1-z}{2}\right)^{j-1} p_{k-1}^{2i+2j-2}(z), \quad \forall i \geq 2, j,k \geq 1. \end{aligned} \tag{4.16}$$

Proof. The results (4.12) are a direct consequence of the relation $\nabla \cdot \nabla\times \equiv 0$. In order to prove (4.16), we observe that in general $\operatorname{div}\big(h(z)\nabla f(x,y,z) \times \nabla g(y,z)\big) = \frac{\partial f}{\partial x}(x,y,z)\frac{\partial g}{\partial y}(y,z)h'(z)$. Therefore, we can conclude

$$\nabla \cdot \widetilde{\psi}_{ijk}^{(c)}(x,y,z) = \frac{\partial u_i}{\partial x}(x,y,z)\frac{\partial v_{ij}}{\partial y}(y,z)\frac{\partial w_{ijk}}{\partial z}(z).$$

This proves the assertion. For the proof of (4.14) and (4.15), the Nédélec function and the Raviart-Thomas function have to be computed. Simple calculations show

$$\varphi_0^{[1,2]}(x,y,z) = -\frac{1}{8}\begin{bmatrix} 1-2y-z \\ 2x \\ x \end{bmatrix} \quad \text{and} \quad \psi_0^{[1,2,3]}(x,y,z) = \frac{1}{8}\begin{bmatrix} -x \\ -y \\ 1-z \end{bmatrix}. \tag{4.17}$$

A rewriting using (2.5) as in the proof of Lemma 3.3 yields the result. □

Remark 4.3. *As in the two-dimensional case, the results* (4.14), (4.15)*, can be viewed as special cases of* (4.16) *with* $i = 1$*,* $j = 0$ *and* $i = 1$*, respectively.*

Let us define the element stiffness matrix with respect to the basis $[\Psi]$ by

$$\widehat{A} = \int_{\hat{\triangle}} [\nabla \cdot \Psi]^\top \, [\nabla \cdot \Psi] \, \mathrm{d}(x,y,z) := a_{\mathrm{div}}([\Psi],[\Psi]). \tag{4.18}$$

Since the higher-order kernel of the divergence operator is explicitly represented by $[\Psi^F]$ and $[\Psi_1]$ within in the basis $[\Psi]$, the corresponding blocks of the stiffness matrix $\widehat{A}$ are zero by construction. Moreover, the orthogonality properties of the remaining shape functions $[\Psi]$ are as follows.

Theorem 4.4. *Let the set* $[\Psi]$ *of basis functions be defined in* (4.9)*. Then, the fluxes* $[\nabla \cdot \Psi_I]$ *are* L_2*-orthogonal to* $[\nabla \cdot \Psi]$*. Moreover, the stiffness matrix* $\widehat{A}$ *defined in* (4.18) *is diagonal up to the* 4×4 *low-order block* $a_{\mathrm{div}}([\Psi_0],[\Psi_0])$*.*

Proof. With the closed forms given in Lemma 4.2, the assertion follows by simple calculations. By (4.16) the divergence of $\widetilde{\psi}^{(c)}_{ijk}$ are just the $L_2(\hat{\Delta})$-orthogonal basis functions and their inner product is given by

$$\left(\nabla \cdot \widetilde{\psi}^{(c)}_{ijk}, \nabla \cdot \widetilde{\psi}^{(c)}_{lmn}\right) = \frac{4\delta_{i,l}\delta_{j,m}\delta_{k,n}}{(2i-1)(i+j-1)(2i+2j+2k-3)},$$

see [31]. After performing the Duffy transformation we obtain for the remaining products with $\widetilde{\psi}^{(c)}_{ijk}$ that

$$\left(\nabla \cdot \widetilde{\psi}^{(c)}_{ijk}, \nabla \cdot \widetilde{\psi}^{(b)}_{1mn}\right) = \int_{-1}^{1} 1 \cdot p^0_{i-1} \,\mathrm{d}x * \text{further integrals} = 0,$$

$$\left(\nabla \cdot \widetilde{\psi}^{(c)}_{ijk}, \nabla \cdot \widetilde{\psi}^{(a)}_{10n}\right) = \int_{-1}^{1} 1 \cdot p^0_{i-1} \,\mathrm{d}x * \text{further integrals} = 0,$$

since $i \geq 2$. Furthermore, we have,

$$\begin{aligned}\left(\nabla \cdot \widetilde{\psi}^{(b)}_{1jk}, \nabla \cdot \widetilde{\psi}^{(b)}_{1mn}\right) &= \frac{1}{4}\int_{-1}^{1} \frac{1-y}{2} p^1_j(y) p^1_m(y) \,\mathrm{d}y \int_{-1}^{1} \left(\frac{1-z}{2}\right)^{j+m+2} p^{2j+2}_{k-1}(z) p^{2m+2}_{n-1}(z) \,\mathrm{d}z \\ &= \frac{\delta_{j,m}\delta_{k,n}}{2(j+1)(2k+2j+1)}.\end{aligned}$$

Since $j \geq 1$, we can conclude

$$\left(\nabla \cdot \widetilde{\psi}^{(b)}_{1jk}, \nabla \cdot \widetilde{\psi}^{(a)}_{10n}\right) = \frac{1}{8}\int_{-1}^{1} \frac{1-y}{2} p^1_j(y) \,\mathrm{d}y \int_{-1}^{1} \left(\frac{1-z}{2}\right)^{j+2} p^{2j+2}_{k-1}(z) p^2_n(z) \,\mathrm{d}z = 0, \quad (j \geq 1).$$

Finally, we have

$$\left(\nabla \cdot \widetilde{\psi}^{(a)}_{10k}, \nabla \cdot \widetilde{\psi}^{(a)}_{10n}\right) = \frac{1}{8}\int_{-1}^{1} \left(\frac{1-z}{2}\right)^{2} p^2_k(z) p^2_n(z) \,\mathrm{d}z = \frac{\delta_{k,n}}{4(2k+3)}.$$

This completes the proof. □

Remark 4.5. *The special choice* (4.11) *of the auxiliary functions implies that the fluxes* $\{1/|\hat{\triangle}|, \nabla \cdot \Psi_2\}$ *of the non-solenoidal shape functions coincide with the* L_2*-orthogonal Dubiner basis for the* L_2*-conforming tetrahedron as presented in [31].*

Next, the sparsity of the element mass matrix block, i.e.

$$\widehat{M}_{II} = \int_{\hat{\Delta}} [\Psi_I]^\top \, [\Psi_I] \,\mathrm{d}(x,y,z), \tag{4.19}$$

is investigated. It can be shown that the number of nonzero entries per row in the block $\widehat{M}_{II}$ is $\mathcal{O}(1)$ and hence independent of the polynomial degree p. Since the number of combinations as well as the integrals to be computed in the sparsity proof of the mass matrix become very involved, we do not evaluate them by hand, but utilize the algorithm and implementation presented in [8, 9]. An upper bound for the non-zero entries is summarized in the following lemma.

Lemma 4.6. *Let* $[\Psi_I]$ *be the set of interior shape functions on the reference tetrahedron* $\hat{\triangle}$ *(of polynomial order* p*) as defined in* (4.8)*. Then the number of nonzero entries per row in the matrix* $\widehat{M}_{II}$ *is bounded by a constant independent of the polynomial degree* p*. More precisely, the following implications hold: Let* $i, l \geq 2$ *and* $j, k, m, n \geq 1$*. If* $|i-l| > 2$ *or*

1. $|i-l+j-m|>2$ *or* $|i-l+j-m+k-n|>2$ *then the inner products*

$$\begin{aligned}&\big(\psi^{(a)}_{1jk},\psi^{(a)}_{1mn}\big)_{0,\hat{\triangle}},\big(\psi^{(b)}_{ijk},\psi^{(b)}_{lmn}\big)_{0,\hat{\triangle}},\big(\psi^{(c)}_{ijk},\psi^{(c)}_{lmn}\big)_{0,\hat{\triangle}},\big(\widetilde{\psi}^{(a)}_{10k},\widetilde{\psi}^{(a)}_{10n}\big)_{0,\hat{\triangle}},\big(\widetilde{\psi}^{(b)}_{1jk},\widetilde{\psi}^{(b)}_{1mn}\big)_{0,\hat{\triangle}},\\&\big(\widetilde{\psi}^{(c)}_{ijk},\widetilde{\psi}^{(c)}_{lmn}\big)_{0,\hat{\triangle}},\big(\psi^{(a)}_{1jk},\widetilde{\psi}^{(b)}_{1mn}\big)_{0,\hat{\triangle}},\big(\widetilde{\psi}^{(b)}_{1jk},\psi^{(a)}_{1mn}\big)_{0,\hat{\triangle}},\big(\psi^{(b)}_{ijk},\psi^{(c)}_{lmn}\big)_{0,\hat{\triangle}},\big(\psi^{(c)}_{ijk},\psi^{(b)}_{lmn}\big)_{0,\hat{\triangle}},\\&\big(\psi^{(b)}_{ijk},\widetilde{\psi}^{(c)}_{lmn}\big)_{0,\hat{\triangle}},\big(\widetilde{\psi}^{(c)}_{ijk},\psi^{(b)}_{lmn}\big)_{0,\hat{\triangle}},\big(\psi^{(c)}_{ijk},\widetilde{\psi}^{(c)}_{lmn}\big)_{0,\hat{\triangle}},\big(\widetilde{\psi}^{(c)}_{ijk},\psi^{(c)}_{lmn}\big)_{0,\hat{\triangle}},\end{aligned}$$

vanish.

2. $|i-l+j-m+1|>2$ *or* $|i-l+j-m+k-n+1|>2$ *then the inner products*

$$\begin{aligned}&\big(\psi^{(a)}_{1jk},\psi^{(b)}_{lmn}\big)_{0,\hat{\triangle}},\big(\psi^{(a)}_{1jk},\psi^{(c)}_{lmn}\big)_{0,\hat{\triangle}},\big(\psi^{(a)}_{1jk},\widetilde{\psi}^{(c)}_{lmn}\big)_{0,\hat{\triangle}},\big(\widetilde{\psi}^{(a)}_{10k},\psi^{(a)}_{1mn}\big)_{0,\hat{\triangle}},\\&\big(\widetilde{\psi}^{(a)}_{10k},\widetilde{\psi}^{(b)}_{1mn}\big)_{0,\hat{\triangle}},\big(\widetilde{\psi}^{(b)}_{1jk},\psi^{(b)}_{lmn}\big)_{0,\hat{\triangle}},\big(\widetilde{\psi}^{(b)}_{1jk},\psi^{(c)}_{lmn}\big)_{0,\hat{\triangle}},\big(\widetilde{\psi}^{(b)}_{1jk},\widetilde{\psi}^{(c)}_{lmn}\big)_{0,\hat{\triangle}}\end{aligned}$$

vanish.

3. $|i-l+j-m-1|>2$ *or* $|i-l+j-m+k-n-1|>2$ *then the inner products*

$$\begin{aligned}&\big(\psi^{(b)}_{ijk},\psi^{(a)}_{1mn}\big)_{0,\hat{\triangle}},\big(\psi^{(c)}_{ijk},\psi^{(a)}_{1mn}\big)_{0,\hat{\triangle}},\big(\widetilde{\psi}^{(c)}_{ijk},\psi^{(a)}_{1mn}\big)_{0,\hat{\triangle}},\big(\psi^{(a)}_{1jk},\widetilde{\psi}^{(a)}_{10n}\big)_{0,\hat{\triangle}},\\&\big(\widetilde{\psi}^{(b)}_{1jk},\widetilde{\psi}^{(a)}_{10n}\big)_{0,\hat{\triangle}},\big(\psi^{(b)}_{ijk},\widetilde{\psi}^{(b)}_{1mn}\big)_{0,\hat{\triangle}},\big(\psi^{(c)}_{ijk},\widetilde{\psi}^{(b)}_{1mn}\big)_{0,\hat{\triangle}},\big(\widetilde{\psi}^{(c)}_{ijk},\widetilde{\psi}^{(b)}_{1mn}\big)_{0,\hat{\triangle}}\end{aligned}$$

vanish.

4. $|i-l+j-m-1|>2$ *or* $|i-l+j-m+k-n-2|>2$ *then* $\big(\psi^{(b)}_{ijk},\widetilde{\psi}^{(a)}_{10n}\big)_{0,\hat{\triangle}}=0$ *and* $\big(\widetilde{\psi}^{(c)}_{ijk},\widetilde{\psi}^{(a)}_{10n}\big)_{0,\hat{\triangle}}=0$.

5. $|i-l+j-m+1|>2$ *or* $|i-l+j-m+k-n+2|>2$ *then* $\big(\widetilde{\psi}^{(a)}_{10k},\psi^{(b)}_{lmn}\big)_{0,\hat{\triangle}}=0$ *and* $\big(\widetilde{\psi}^{(a)}_{10k},\widetilde{\psi}^{(c)}_{lmn}\big)_{0,\hat{\triangle}}=0$.

6. $\big(\psi^{(c)}_{ijk},\widetilde{\psi}^{(a)}_{10n}\big)_{0,\hat{\triangle}}=0$ *and* $\big(\widetilde{\psi}^{(a)}_{10k},\psi^{(c)}_{lmn}\big)_{0,\hat{\triangle}}=0$.

Proof. Evaluation of the integrals using the algorithm introduced in [8, 9]. □

Remark 4.7. *Note that the sparsity pattern as stated in Lemma 4.6 only gives an* upper *bound for the number of nonzero entries in the mass matrix to simplify the presentation. In Appendix B we give a short summary of the applied algorithm and sketch the proof of the sparsity result on the reference tetrahedron* $\hat{\triangle}$ *as depicted in Figure 1 for the part* $\big(\widetilde{\psi}^{(c)}_{ijk},\widetilde{\psi}^{(c)}_{lmn}\big)_{0,\hat{\triangle}}$. *It is also for this element that the mass matrix becomes least populated. The essential difference between this reference tetrehadron and an arbitrarily chosen is that the branches* $|i-l|=1$ *are vanishing on* $\hat{\triangle}$ *due to geometric symmetries of the reference element. The complete information on the sparsity pattern of the inner block of the mass matrix as well as precomputed matrix entries for arbitrary tetrahedra (in terms of barycentric coordinates) can be found at*

`http://www.risc.jku.at/people/vpillwei/hdiv/` .

5 The global matrix

The nonzero pattern of the element matrices has been considered in the previous two sections for the two-dimensional and three-dimensional case, respectively. In this section, we investigate the global matrix

$$\mathcal{K}_{\mathbf{\Psi}} := a([\mathbf{\Psi}],[\mathbf{\Psi}]) \quad \text{with} \quad a(u,v) := (\kappa\nabla\cdot u,\nabla\cdot v)+(\varepsilon u,v) \tag{5.1}$$

which can be represented by the local element matrices, i.e.,

$$\mathcal{K}_{\mathbf{\Psi}} = \sum_{s=1}^{nel} R_s^\top K_s R_s, \tag{5.2}$$

where K_s are the local matrices on Δ_s and R_s are the usual finite element connectivity matrices, *nel* denotes the number of elements and $[\mathbf{\Psi}]$ is the global basis. First, the authors have a look to the structure of the local matrices on the elements where the Piola-transformation is required.

5.1 The Piola transformation for general simplices

The conforming mapping of $H(\mathrm{div})$-conforming basis functions requires the Piola transformation (cf. [12, 23]). Let $\triangle_s$ be a non-degenerated simplex in $\mathbb{R}^d$, $d = 2, 3$ and $\hat{\triangle}$ be the reference simplex depicted in Figure 1, respectively. Let $F_s : \hat{\triangle} \to \triangle_s$ be the bijective element mapping with Jacobian DF_s and Jacobi determinant $J_s := \det(DF_s)$. The *Piola transformation* of a function $\hat{\psi} \in H(\mathrm{div}, \hat{\triangle})$ is defined by

$$\psi\,|_{\triangle_s} = J_s^{-1}\,(DF_s)^T \hat{\psi} \circ F_s^{-1}. \tag{5.3}$$

Then there holds $\psi \in H(\mathrm{div}, \triangle_s)$ with

$$\nabla \cdot \psi\,|_{\triangle_s} = {J_s}^{-1}\,\hat{\nabla} \cdot \hat{\psi} \circ F_s^{-1}. \tag{5.4}$$

The Piola transformation is kernel preserving [18], hence the Piola mapping of a divergence-free function is divergence-free.
The basis functions for general (possibly curved) simplicial elements can be defined via the Piola transformation. Let $[\Psi]$ denote the basis functions on the reference element $\hat{\triangle}$ and $[\Psi_s] := J_s^{-1}\,(DF_s)^T[\Psi] \circ F_s^{-1}$ its Piola transformation. Let us define the element matrices corresponding to an element $\triangle_s$ as

$$A_s = \int_{\Delta_s} (\nabla \cdot [\Psi_s])^\top \ \nabla \cdot [\Psi_s]\ \mathrm{d}(x,y,z) \quad \text{and} \quad M_s = \int_{\Delta_s} [\Psi_s]^\top\ [\Psi_s]\ \mathrm{d}(x,y,z) \tag{5.5}$$

5.2 Sparsity results for affine linear mapping and piecewise constant coefficients

For general (affine) simplices the Piola mapping $[\Psi_s]$ coincides with the basis functions (3.9) and (4.9) defined in barycentric coordinates, for $d = 2, 3$, respectively. The Piola mapping allows us to generalize the orthogonality results stated in Theorem 4.4 and Lemma 4.6 (Theorem 3.6 and Lemma 3.8 in the 2D-case) for the reference element to general affine simplices.

Lemma 5.1. *Let F_s be an affine element mapping and A_s and M_s be defined by* (5.5)*. Then, the element stiffness matrix A_s, as defined in* (5.5)*, is diagonal up to the $(d+1) \times (d+1)$ low-order block. Moreover, the interior block $M_{II}^{(s)}$ of the element mass matrix M_s is sparse having only $\mathcal{O}(p^d)$ nonzero entries.*

Proof. For affine element transformations the Piola transformation of the divergence (5.4) simplifies to scaling by a constant, i.e. the orthogonality relations of fluxes and sparsity properties of the stiffness matrix $\hat{A}$ obviously generalizes onto general affine simplices.
The sparsity result for the mass matrix relies on affine transformations, where we refer the interested reader to the appendix of this technical report. □

Finally, we investigate the properties of the global system matrix $\mathcal{K}_{\mathbf{\Psi}}$ assuming triangulations with affine simplices Δ_s and piecewise constant coefficients $\kappa(x)\,|_{\Delta_s} = \kappa_s$ and $\varepsilon(x)\,|_{\Delta_s} = \varepsilon_s$. We denote the global stiffness and mass matrix as

$$\mathcal{A}_{\mathbf{\Psi}} = \sum_{s=1}^{nel} \varepsilon_s R_s^\top A_s R_s \quad \text{and} \quad \mathcal{M}_{\mathbf{\Psi}} = \sum_{s=1}^{nel} \kappa_s R_s^\top M_s R_s. \tag{5.6}$$

The sparsity results of Theorem 4.4, Lemma 4.6 (Theorem 3.6 and Lemma 3.8 in the 2D-case) and the relation $K_s = \varepsilon_s A_s + \kappa_s M_s$ (due to (1.3)) immediately imply global sparsity as summarized in the next theorem.

Theorem 5.2. *Let $\mathcal{K}_{\mathbf{\Psi}}$, $\mathcal{A}_{\mathbf{\Psi}}$ and $\mathcal{M}_{\mathbf{\Psi}}$ be defined by (5.1) and (5.6), respectively. Let $[\Psi]$ be partitioned into coupling (denoted by C), i.e. low-order and face-based, basis functions, and element-based interior (denoted by I) basis functions, then the global matrix $\mathcal{K}_{\mathbf{\Psi}}$ can be written in the form*

$$\mathcal{K}_{\mathbf{\Psi}} = \begin{bmatrix} \mathcal{K}_{CC} & \mathcal{K}_{CI} \\ \mathcal{K}_{IC} & \mathcal{K}_{II} \end{bmatrix}$$

Let $\mathcal{A}_{\mathbf{\Psi}}$ and $\mathcal{M}_{\mathbf{\Psi}}$ be partitioned the same way. Then the following assertions hold:

- *The inner diagonal block $\mathcal{M}_{II}$ of the global mass matrix and the inner diagonal block $\mathcal{K}_{II}$ of the system matrix are sparse with $\mathcal{O}(nel\, p^d)$ total nonzero entries.*

Furthermore, the global stiffness matrix reduces to the form

$$\mathcal{A}_{\mathbf{\Psi}} = \begin{bmatrix} \mathcal{A}_{CC} & \mathbf{0} \\ \mathbf{0} & \mathcal{A}_{II} \end{bmatrix} \qquad \text{with coupling block } \mathcal{A}_{CC} = \begin{pmatrix} \mathcal{A}_{00} & \mathbf{0} \\ \mathbf{0} & \mathbf{0} \end{pmatrix}$$

- *with inner block $\mathcal{A}_{II}$ being a diagonal matrix and*
- *sparse low-order stiffness matrix $\mathcal{A}_{00}$ with $\mathcal{O}(nel)$ total nonzero entries.*

Fast Assembling strategies of system matrices
There are two alternative ways of efficiently assembling the system matrices $\mathcal{K}_{\psi}$. The new set of basis functions (3.1)-(3.7) apply by construction two both variants of fast assembling.
(i) Recursive evaluation of matrix entries: All matrix entries can be evaluated recursively, cf. [26], with a total cost or $\mathcal{O}(p^d)$ operations for the matrix.
(ii) Sum factorization: The basis functions (3.1)-(3.7) on the reference triangle are the result of one-dimensional basis functions under the Duffy-transformation. Using sum factorization techniques, [22], [20], the generation of $\mathcal{K}_{\mathbf{\Psi}}$ can be performed in $\mathcal{O}(p^3)$ operations for $d = 2, 3$, respectively. The algorithm is presented in the Appendix C.

6 Numerical experiments

In this chapter we investigate practically achieved sparsity patterns and condition numbers of the finite element system matrix using the proposed mixed-weighted Jacobi-type finite element basis functions in several settings.

6.1 Sparsity pattern for triangular elements

Sparsity pattern of element matrices on the reference triangle In Figure 2 the sparsity pattern of the stiffness and mass matrix for the FE basis (3.1)-(3.7) for uniform polynomial order $p = 25$ is visualized. The inner block $\widehat{M}_{II}$ (3.15) according to all interior basis functions (3.8) is sparse. In fact, due to further orthogonality properties caused by the special geometric properties of the reference triangle the sparsity pattern for this geometry is even better than proven in Lemma 3.8. The element stiffness matrix $\widehat{A}$ is diagonal up to a 3×3 low-order block (which is not visible on the used scale).

Interior coupling of facet-based degree's of freedom The second plot of Figure 2 shows the element mass matrix including all degrees of freedom, i.e. low-order, edge-based and cell-based ones. Obviously, the block $\widehat{M}_{CI}$ is in general non-sparse having $\mathcal{O}(p^{d-1})$ nonzero entries per row, an analogue result is obtained in 3d. This is due to the used monomial extension of polynomial

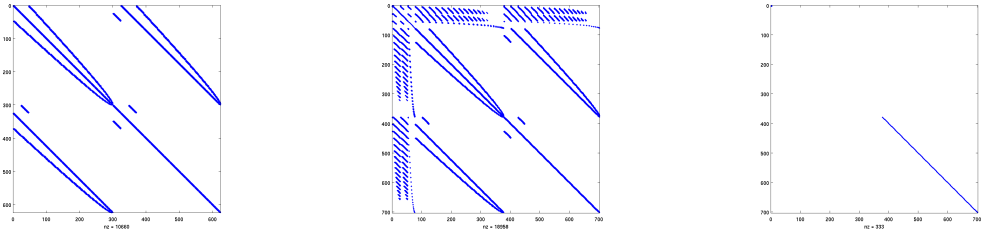

Figure 2: Sparsity pattern for polynomial order $p = 25$ on reference triangle $\hat{\triangle}$: inner block $\widehat{M}^{II}$ of mass matrix (left), mass matrix $\widehat{M}$ with facet-coupling terms (middle) and element stiffness matrix $\widehat{A}$ (right).

normal traces into the interior (based on Duffy's transformation) in the definition of facet-based shape functions (3.2) and (3.3). This construction can be optimal only for one edge: the one for which the Duffy transformation used for extending edge-traces into the interior coincides with the Duffy transformation used for the interior basis functions (3.8), i.e. the third edge in the example used for Figure 2.

Remark 6.1. *The matrix blocks $\mathcal{M}_{CC}$ and $\mathcal{M}_{CI}$ can be factorized into a product of sparse matrices, as done for H^1-conforming problems in [8] and [10] for 3d, but the advantages get visible only for very high polynomial order p.*

The remedy to this problem would be the use of $H(\mathrm{div})$-conforming facet-based shape functions with optimal extension into the interior, but this is (up to the knowledge of the authors) an open problem. Nevertheless, results on optimal extensions for H^1-conforming basis functions can be found in [7].

6.2 Numerical results for reference, affine and curved tetrahedra

The choice of the basis functions (4.1)-(4.9) follows the general construction principle of $H(\mathrm{div})$-conforming basis functions suggested in [35]: combining a hierarchic construction using warped tensor-products of orthogonal polynomials and the explicit use of solenoidal basis functions expressed in proper combinations of tensor-products and differential fields of three sets of auxiliary functions u_i, v_{ij} and w_{ijk}. The main contribution of the new shape functions is (i) the careful choice of the auxiliary functions (4.7) and respectively (4.2) based on Jacobi-type polynomials with properly chosen mixed-weights, and (ii) the proper choices (with respect to mixed-weights) of auxiliary functions in the shape functions labeled by the superscripts (a) and (b) in (4.5) and (4.6). In the following, we want to compare the introduced shape functions with a commonly-used non-weighted Legendre-type shape functions.

Legendre-type H(div)-conforming shape functions In order to demonstrate the impact of using mixed-weighted Jacobi-polynomials we numerically compare sparsity and condition numbers implied by the new FE basis with a basis using the low-order shape functions (4.3), but auxiliary functions based on Legendre-type polynomials, namely

$$\begin{aligned} u_i = u_i^L &:= \hat{p}_i^0\left(\frac{\lambda_2-\lambda_1}{\lambda_2+\lambda_1}\right)(\lambda_2+\lambda_1)^i, \\ v_{ij} = v_j^L &:= \lambda_3 p_{j-1}^0\left(\frac{2\lambda_3-(1-\lambda_4)}{1-\lambda_4}\right)(1-\lambda_4)^{j-1}, \\ \text{and} \quad w_{ijk} = w_k^L &:= \lambda_4 p_{k-1}^0(2\lambda_4-1), \end{aligned} \tag{6.1}$$

for $i \geq 2, j \geq 1, k \geq 1$, in the definition of the face-based shape functions (4.1) as well as in the cell-based shape (4.6). This yields a commonly used choice of $H(\mathrm{div})$-conforming basis functions. The orthogonality properties of the Legendre polynomials also imply a sparsity pattern for system matrices based on Legendre-type $H(\mathrm{div})$-conforming basis functions. We refer the interested reader to the Appendix D.
In the remaining part of this section, we will compare practically achieved sparsity patterns and condition numbers using Jacobi-type auxiliary functions (4.2) and (4.7) in contrast to above Legendre-type auxiliary functions first, on the reference tetrahedron, secondly on the general affine tetrahedron $\triangle_s$ with vertices $(0,0,0)$, $(0.315, 0.632, 0.158)$, $(1.5,0,0)$, and $(0,0,1)$ as well as the eighth of the unit sphere meshed by 4 curved tetrahedral elements. We remark that we always use diagonal preconditioning within the computation of condition numbers.

A comparison of the sparsity pattern on affine tetrahedra Figure 3 shows the sparsity pattern of the element stiffness matrix A_s and the inner block $M_{s,II}$ of the element mass matrix using $H(\mathrm{div})$-conforming properly weighted Jacobi-type shape functions as suggested in Chapter 4. Due to symmetry properties one obtains an improved sparsity pattern for the inner block $\widehat{M}_{II}$ of the element mass matrix on the reference element as shown in the first graph in Figure 3. For the affine tetrahedron $\triangle_s$ one obtains the sparsity pattern as depicted in the second plot. Using Legendre-type auxiliary functions (6.1) one observes sparsity patterns with much more non-zero entries as shown in Figure 3.

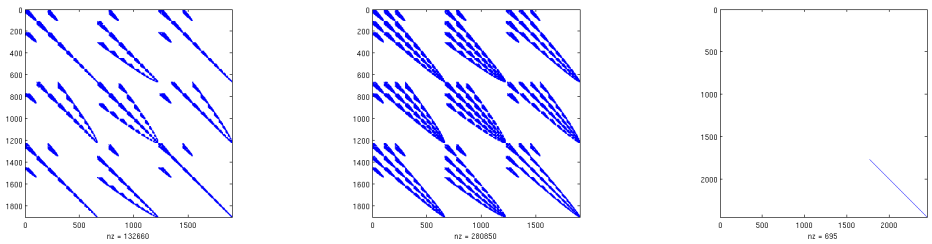

Figure 3: Optimally weighted Jacobi-type basis $[\Psi]$ for $p = 15$: Sparsity pattern of inner block $\widehat{M}_{II}$ of element mass (left) on reference tetrahedron $\hat{\triangle}$, inner block $M_{s,II}$ of mass matrix (middle) and stiffness matrix A_s on a general affine tetrahedron $\triangle_s$.

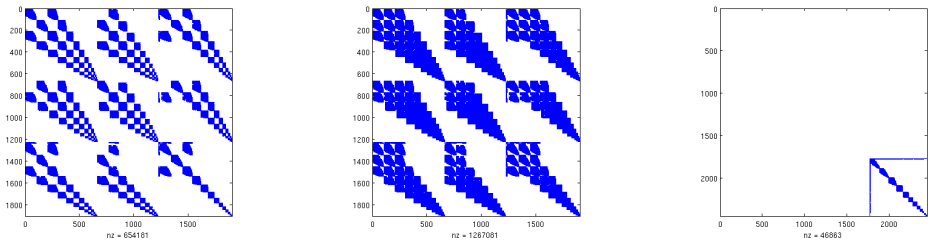

Figure 4: Integrated Legendre-type basis $[\Psi^{Leg}]$ for $p = 15$: Sparsity pattern of inner block $\widehat{M}_{II}^{Leg}$ of element mass (left) on reference tetrahedron $\hat{\triangle}$, inner block $M_{s,II}^{Leg}$ of mass matrix (middle) and stiffness matrix A_s^{Leg} on a general affine tetrahedron $\triangle_s$.

A comparison of condition numbers for the general affine tetrahedra $\triangle_s$ Table 1 shows a comparison of practically achieved condition numbers of the inner block of $K_{s,II} = A_{s,II} + M_{s,II}$

degree	$\kappa(K_{s,II})$	$\kappa(K_{s,II}^{Leg})$
p=3	1.7E+01	3.4E+01
p=5	6.6E+01	1.5E+03
p=8	3.1E+02	1.2E+06
p=10	6.8E+02	2.7E+08
p=13	1.8E+03	1.2E+10
p=15	3.1E+03	
p=20	9.4E+03	

degree	$\kappa(K_{s,II})$	eoc of $\mathcal{O}(p^k)$
p=5	6.6E+01	
p=10	6.8E+02	3.37
p=15	3.1E+03	3.73
p=20	9.4E+03	3.86

Table 1: Practically achieved condition numbers $\kappa(K_{s,II})$ for $K = A + M$ for a general affine tetrahedron Δ_s (left) and experimental order of convergence k according to $\kappa(K_{II}) = \mathcal{O}(p^k)$ for new Jacobi-type basis (right).

on the affine tetrahedron $\triangle_s$ using auxiliary functions with and without properly chosen weights in the construction of $H(\mathrm{div})$-conforming basis functions. One observes that the quality of the condition numbers when increasing polynomial degree p crucially depends on the proper weights in the auxiliary functions, cf. (4.7) and (6.1).
The elimination of inner degrees of freedom via static condensation (see e.g. [20] Section 4.2) is an established tool for the efficient solution of algebraic equation systems arising from p and hp-FE disretizations. The left table of Table 1 shows that for Legendre-type basis functions the condition numbers for the inner blocks deteriorate already for moderate p. Hence, in view of accuracy and reliable digits of the solution the applicability of static condensation gets already critical for polynomial order greater than 8. Contrary to that using properly weighted Jacobi-type auxiliary functions yields much small condition numbers which are still moderate for $p = 20$. Numerical examples indicate that the condition number using mixed-weighted Jacobi-type basis functions depends on the polynomial order sligthly better as $\mathcal{O}(p^4)$.

The parameter-dependent div-div-problem Next, we investigate the dependency of the condition number of the parameter-dependent system matrix $K_s := \kappa A_s + \varepsilon M_s$ corresponding to the parameter-dependent div-div-problem (5.1). Since the matrix A_s is only positive semidefinite with large non-trivial kernel space, parameter-robust preconditioning gets an issue especially for small parameters ε, as analyzed in [4] and [19]. It is shown in [35] that using solenoidal basis functions, namely (4.1) and (4.5), in the construction of the $H(\mathrm{div})$-conforming FE-basis, a parameter-robustness is provided by a parameter-robust preconditioner for the low-order space as e.g. Hiptmair [4] or Arnold-Falk-Winther [19], and simple diagonal preconditioning of the higher-order face-based and cell-based degrees of freedom. Figure shows the condition numbers of the inner block $K_{s,II}$ for $\kappa = 1$ and varying parameter ε from 10^{-5} up to 10^5 which are indeed robust with respect to positive parameters ε.

Application to curved domains Even if the sparsity property of the suggested shape functions gets lost, the improved condition numbers obtained by Jacobi-type auxiliary functions remain for curved element geometries as documented in Table 6. For e.g. $p = 10$ static condensation is reasonable only for the suggested Jacobi-type basis functions, as well as the global system matrix is moderate-conditioned with respect to the polynomial order p and could be further improved by either optimal extension of face-based shape functions or by appropriate splitting techniques as mentioned in Remark 6.1. Already for moderate p the suggested Jacobi-type shape functions yield substant improvements even for general problem settings and curved domains.

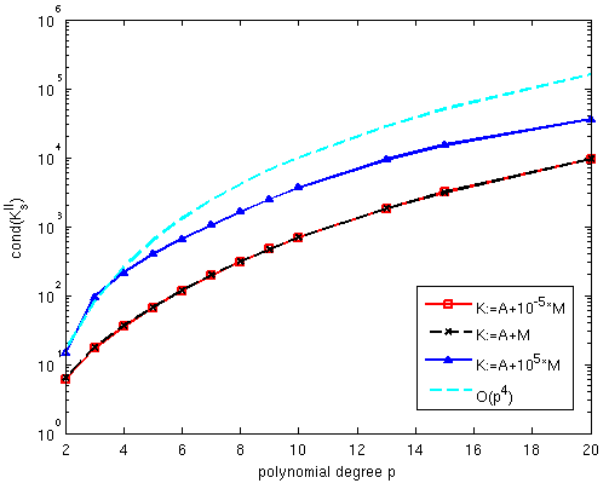

Figure 5: Condition numbers of inner block $K_{s,II}$ (on general tetrahedron) with respect to polynomial order p, for bilinearform $a(u,v) := (\nabla \cdot u, \nabla \cdot v) + \varepsilon(u,v)$ with varying constant coefficient $\varepsilon = 10^{-5}, 1, 10^5$.

	inner blocks		system matrix	
	$\kappa(K_{II})$	$\kappa(K_{II}^{Leg})$	$\kappa(K)$	$\kappa(K^{Leg})$
p=5	3.7E+01	3.5E+03	1.2E+03	2.5E+04
p=10	3.6E+02	9.0E+07	2.0E+04	4.0E+08

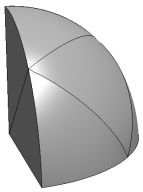

Figure 6: Comparison of condition numbers of inner block and full matrix $K = A + M$ for one eighth of a sphere meshed with 4 curved tetrahedra

A Jacobi polynomials

For the Jacobi polynomials (2.1) and the integrated Jacobi polynomials (2.2) there hold

$$\begin{aligned}
\hat{p}_n^\alpha(-1) &= 0, \quad n \geq 1, && \text{(A.1)}\\
p_n^{\alpha-1}(x) &= \frac{1}{\alpha+2n}\left[(\alpha+n)p_n^\alpha(x) - np_{n-1}^\alpha(x)\right], && \text{(A.2)}\\
\hat{p}_n^\alpha(x) &= \frac{2}{2n+\alpha-1}\left(p_n^{\alpha-1}(x) + p_{n-1}^{\alpha-1}(x)\right), \quad n \geq 1, && \text{(A.3)}\\
\hat{p}_n^\alpha(x) &= \frac{2n+2\alpha}{(2n+\alpha-1)(2n+\alpha)}p_n^\alpha(x) + \frac{2\alpha}{(2n+\alpha-2)(2n+\alpha)}p_{n-1}^\alpha(x)\\
&\quad - \frac{2n-2}{(2n+\alpha-1)(2n+\alpha-2)}p_{n-2}^\alpha(x), \quad n \geq 2, && \text{(A.4)}\\
yp_{j-1}^\alpha(y) - j\hat{p}_j^\alpha(y) &= \frac{1}{2j+\alpha-2}\left(-\alpha p_{j-1}^\alpha(y) + (2j-2)p_{j-2}^\alpha(y)\right), \qquad \alpha > -1, j \geq 2. && \text{(A.5)}
\end{aligned}$$

additionally to the relations (2.4) and (2.5). Formula (A.4) gives a simple connection between the Jacobi and the integrated Jacobi polynomials.
Furthermore, there hold the recurrence relations

$$\begin{aligned}
p_{n+1}^\alpha(x) =& \frac{2n+\alpha+1}{(2n+2)(n+\alpha+1)(2n+\alpha)}\left((2n+\alpha+2)(2n+\alpha)x + \alpha^2\right)p_n^\alpha(x)\\
&- \frac{n(n+\alpha)(2n+\alpha+2)}{(n+1)(n+\alpha+1)(2n+\alpha)}p_{n-1}^\alpha(x), \quad n \geq 1, && \text{(A.6)}\\
\hat{p}_{n+1}^\alpha(x) =& \frac{2n+\alpha-1}{(2n+2)(n+\alpha)(2n+\alpha-2)}\left((2n+\alpha-2)(2n+\alpha)x + \alpha(\alpha-2)\right)\hat{p}_n^\alpha(x)\\
&- \frac{(n-1)(n+\alpha-2)(2n+\alpha)}{(n+1)(n+\alpha)(2n+\alpha-2)}\hat{p}_{n-1}^\alpha(x), \quad n \geq 1. && \text{(A.7)}
\end{aligned}$$

Together with the initial values $p_{-1}^\alpha = 0$, $p_0^\alpha = 1$ or $\hat{p}_{-1}^\alpha = 0$, $\hat{p}_0^\alpha 1$, for $\alpha > 0$, and $\hat{p}_0^0 = -1$ they can be used for fast evaluation of Jacobi and Integrated Jacobi polynomials as needed in the evaluation of the suggested shape functions. The most important results for our work are the formulas (A.4) and (A.6).

B Algorithmic exact evaluation of the integrals

The sparsity pattern for the mass matrix in three dimensions has been summarized in Lemma 4.6 where for the proof the integrals are evaluated exactly using the algorithm presented in [8, 9]. The main concept of this algorithm is a rewriting procedure exploiting relations (A.2)–(A.5) until each term contributing to the integrand can be evaluated using the orthogonality relation (2.4). This procedure terminates with the symbolic evaluation of the integrals, if the result is nonzero for only finitely many combinations of indices and aborts otherwise, returning the integrand up to which evaluation was possible. This of course then allows for adaptive adjustment of the parameters in the construction of the basis functions. For sake of completeness, we sketch the arguments for a specific part of the inner block in the next lemma. Here we omit details like the concrete nature of the coefficients that are usually large rational functions in the polynomial degrees of the basis functions. Note that the assertion on the nonzero pattern in the lemma below is sharper than the upper bound we gave earlier, as indicated already in Remark 4.7.

Lemma B.1. *In the setting of section 4.2 it holds that*

$$(i \neq l \vee |i-l+j-m| > 1 \vee |i-l+j-m+k-n| > 2) \Rightarrow \left(\widetilde{\psi}_{ijk}^{(c)}, \widetilde{\psi}_{lmn}^{(c)}\right)_{0,\hat{\triangle}} = 0.$$

Proof. Using the abbreviatons $r = \frac{1-2y-z}{4}$, $s = \frac{1-z}{2}$ and by means of (A.5) we have

$$(\nabla u_i \times \nabla v_{ij})(x,y,z) = -\frac{r^{i-1}s^{j-1}}{2(2i+2j-3)} \begin{pmatrix} p_{i-2}^0\left(\frac{x}{r}\right)\left((2i+j-2)p_{j-1}^{2i-1}\left(\frac{y}{s}\right) - (j-1)p_{j-2}^{2i-1}\left(\frac{y}{s}\right)\right) \\ p_{i-1}^0\left(\frac{x}{r}\right)\left(2(j-1)p_{j-2}^{2i-1}\left(\frac{y}{s}\right) - (2i-1)p_{j-1}^{2i-1}\left(\frac{y}{s}\right)\right) \\ -2(2i+2j-3)p_{i-1}^0\left(\frac{x}{r}\right)p_{j-1}^{2i-1}\left(\frac{y}{s}\right) \end{pmatrix},$$

for details see [8, Lemma 6.2]. From this representation it is already obvious that the integrals vanish if $i \neq l$ because of the orthogonality of Legendre polynomials $p_n^0(x)$ with respect to the L_2 inner product.
For the evaluation of the integrals with respect to y, note that after performing the Duffy substitution the factor r^{i+l-2} of the product $\widetilde{\psi}_{ijk}^{(c)} \cdot \widetilde{\psi}_{lmn}^{(c)}$ turns into $\left(\frac{1-y}{2}\right)^{i+l-1}$. Thus in the next step we need to consider integrals of the form

$$\int_{-1}^{1} \left(\frac{1-y}{2}\right)^{2i-1} p_{j-j_1}^{2i-1}(y) p_{m-m_1}^{2i-1} \,\mathrm{d}y, \quad j_1, m_1 \in \{1,2\}.$$

But this is just the inner product with respect to which Jacobi polynomials $p_n^{2i-1}(y)$ are orthogonal, thus yielding an offset of $|j-m| > 1$.
The remaining three integrands to be considered in the final step are

$$I_1 = \left(\tfrac{1-z}{2}\right)^{\gamma-3} \hat{p}_k^{\gamma-2}(z)\hat{p}_n^{\gamma-4}(z),\ I_2 = \left(\tfrac{1-z}{2}\right)^{\gamma-2} \hat{p}_k^{\gamma-2}(z)\hat{p}_n^{\gamma-2}(z),\ I_3 = \left(\tfrac{1-z}{2}\right)^{-1+\gamma} \hat{p}_k^{\gamma-2}(z)\hat{p}_n^{\gamma}(z),$$

where $\gamma = 2i+2j$. In order to invoke the Jacobi orthogonality relation several rewritings are in place. The easiest case is I_2, where it suffices to rewrite integrated Jacobi polynomials in terms of Jacobi polynomials with the same parameter α using (A.4). For I_1 and I_3 firstly integrated Jacobi polynomials $\hat{p}^{\gamma-2}(z)$ and $\hat{p}^{\gamma}(z)$, respectively, are rewritten using (A.3), which drops the parameter α by one thus adjusting to the appearing weight function. Secondly $\hat{p}_n^{\gamma-4}(z)$ and $\hat{p}_n^{\gamma-2}(z)$ are transformed using (A.4) to obtain Jacobi polynomials and then adjusted to the weight function using (A.2). Each of these steps introduces up to two additional shifts in the polynomial degrees. Since none of the contributions cancel in general this yields the nonzero pattern as stated above. □

C Fast integration of the stiffness and mass matrix

C.1 Sum Factorization

In this section, we present an algorithm for the fast numerical generation of the local element matrices A_s and M_s (5.5) for tetrahedra. The methods are based on fast summation techniques presented in [22], [20] and are explained for the example of the matrix

$$\hat{\mathcal{I}}^{(6)} = (m_{ijk,i'j'k'})_{i+j+k\leq p, i'+j'+k'\leq p} \tag{C.1}$$

with

$$\begin{aligned} m_{ijk,i'j'k'} \quad = \quad & \int_{\hat{\triangle}} \hat{p}_i^0\left(\frac{4x}{1-2y-z}\right)\hat{p}_{i'}^0\left(\frac{4x}{1-2y-z}\right)\left(\frac{1-2y-z}{4}\right)^{i+i'} \\ & \times \hat{p}_j^{2i-1}\left(\frac{2y}{1-z}\right)\hat{p}_{j'}^{2i'-1}\left(\frac{2y}{1-z}\right)\left(\frac{1-z}{2}\right)^{j+j'} \\ & \times p_k^{2i+2j-2}(z) p_{k'}^{2i'+2j'-2}(z)\,\mathrm{d}(x,y,z). \end{aligned}$$

This matrix is one ingredient $u_i v_{ij} w'_{ijk}$ for the generation of the mass matrix M_s and is identical to the term $\hat{\mathcal{I}}^{(6)}$ in [8]. Due to [8], this matrix has the sparsity pattern

$$m_{ijk,i'j'k'} = 0 \quad \text{if } (i,j,k,i',j',k') \in \mathfrak{S}^p(ijk,i'j'k') \tag{C.2}$$

where

$$\mathfrak{S}^p(ijk,i'j'k') = \{i+j+k \le p, i'+j'+k' \le p, |i-i'| > 2 \vee |i-i'+j-j'| > 4 \\ \vee |i-i'+j-j'+k-k'| > 4\} \tag{C.3}$$

cf. [8]. The Duffy transformation applied to (C.1) gives

$$\begin{aligned} m_{ijk,i'j'k'} &= \int_{-1}^{1} \hat{p}_i^0(x)\hat{\rho}_{i'}^0(x)\,\mathrm{d}x \int_{-1}^{1} \left(\frac{1-y}{2}\right)^{i+i'+1} \hat{p}_{j'}^{2i'-1}(y)\hat{p}_j^{2i-1}(y)\,\mathrm{d}y \\ &\quad \times \int_{-1}^{1} \left(\frac{1-z}{2}\right)^{i+j+i'+j'+2} p_k^{2i+2j-2}(z)p_{k'}^{2i'+2j'-2}(z)\,\mathrm{d}z. \end{aligned} \tag{C.4}$$

All one dimensional integrals are computed numerically by a Gaussian quadrature rule with points x_k, $k = 1,\dots,p+1$ and corresponding weights ω_k. The points and weights are chosen such that

$$\int_{-1}^{1} f(x)\,\mathrm{d}x = \sum_{l=1}^{p+1} \omega_l f(x_l) \quad \forall f \in \mathcal{P}_{2p}. \tag{C.5}$$

Since only polynomials of maximal degree $2p$ are integrated in (C.4), the integrals (C.4) are evaluated exactly. Therefore, we have to compute

$$\begin{aligned} m_{ijk,i'j'k'} &= \sum_{l=1}^{p+1} \omega_l \hat{p}_i^0(x_l)\hat{p}_{i'}^0(x_l) \\ &\quad \times \sum_{m=1}^{p+1} \omega_m \left(\frac{1-x_m}{2}\right)^{i+i'+1} \hat{p}_{j'}^{2i'-1}(x_m)\hat{p}_j^{2i-1}(x_m) \\ &\quad \times \sum_{n=1}^{p+1} \omega_n \left(\frac{1-x_n}{2}\right)^{i+j+i'+j'+2} p_k^{2i+2j-2}(x_n)p_{k'}^{2i'+2j'-2}(x_n), \end{aligned}$$

i.e. for all $(i,j,k,i',j',k') \notin \mathfrak{S}^p(ijk,i'j'k')$, cf. (C.3), (C.2). This is done by the following algorithm.

Algorithm C.1. *1. Compute*

$$h_{i;i'}^{(1)} = \sum_{l=1}^{p+1} \omega_l \hat{p}_i^0(x_l)\hat{p}_{i'}^0(x_l)$$

for all $i,i' \in \mathbb{N}$ satisfying $|i-i'| \le 2$ and $i,i' \le p$.

2. Compute

$$h_{i,j;i',j'}^{(2)} = \sum_{m=1}^{p+1} \omega_m \left(\frac{1-x_m}{2}\right)^{i+i'+1} \hat{p}_j^{2i-1}(x_m)\hat{p}_{j'}^{2i'-1}(x_m)$$

for all $i,j,i',j' \in \mathbb{N}$ satisfying $|i-i'| \le 2$, $|i+j-i'-j'| \le 4$, $i+j \le p$ and $i'+j' \le p$.

3. Compute

$$h_{\beta,k;\beta,'k'}^{(3)} = \sum_{n=1}^{p+1} \omega_n \left(\frac{1-x_n}{2}\right)^{\beta+\beta'+2} p_k^{2\beta-2}(x_n)p_{k'}^{2\beta'-2}(x_n)$$

for all $k,k',\beta,\beta' \in \mathbb{N}$ satisfying $|\beta-\beta'| \le 4$, $|\beta+k-\beta'-k'| \le 4$, $\beta+k \le p$ and $\beta'+k' \le p$.

4. For all $(i,j,k,i',j',k') \notin \mathfrak{S}^p(ijk,i'j'k')$, set

$$m_{ijk,i'j'k'} = h_{i;i'}^{(1)} h_{i,j;i',j'}^{(2)} h_{i+j,k;i'+j',k'}^{(3)}.$$

The algorithm requires numerical evaluation of Jacobi and integrated Jacobi polynomials at the Gaussian points x_l, $l = 1,\dots,p+1$. In the next subsection, we present an algorithm which computes the required values $\hat{p}_k^\alpha(x_l)$, $m = 1,\dots,p+1$, $k = 1,\dots,p$, $\alpha = 1,\dots,2p$ in $\mathcal{O}(p^3)$ operations.

C.2 Fast Evaluation of integrated Jacobi polynomials

The integrated Jacobi polynomials needed in the computation of $m_{ijk,i'j'k'}$ (C.1) are $\hat{p}_i^0(x), \hat{p}_j^{2i-1}(x)$ (progressing in odd steps w.r.t. the parameter α) and $\hat{p}_k^{2i+2j-2}(x)$ (progressing in even steps w.r.t. the parameter α). For $i+j+k \le p$ with $i \ge 2$ and $j,k \ge 1$ this means that

$$[\hat{p}_i^0(x)]_{2\le i\le p}, [\hat{p}_j^3(x)]_{1\le j\le p}, \ldots, [\hat{p}_j^{2p-3}(x)]_{1\le j\le p}, [\hat{p}_k^4(x)]_{1\le k\le p}, \ldots, [\hat{p}_k^{2p-4}(x)]_{1\le k\le p}$$

are needed. Since one group proceeds in even, the other one in odd steps, the total of integrated Jacobi polynomials that are needed is

$$\hat{p}_n^a(x), \qquad 1 \le n \le p-3, \quad 3 \le a \le 2p-3,$$

if we consider the integrated Legendre polynomials separately. However, integrating over identity (A.2) yields

$$\hat{p}_{n+1}^{\alpha-1}(x) = \frac{1}{2n+\alpha}\left((n+\alpha)\hat{p}_{n+1}^{\alpha}(x) - n\hat{p}_n^{\alpha}(x)\right),$$

valid for all $n \ge 0$. Using this relation starting from the integrated Jacobi polynomials of highest degree, i.e. $\alpha = 2i-1 = 2p-3$, the remaining Jacobi polynomials can be computed using only two elements of the previous row. Note that for the initial values $n=1$ we have $\hat{p}_1^{\alpha}(x) = 1+x$ for all α. For assembling the polynomials of highest degree the three term recurrence (A.7) is used. Summarizing, the evaluation of the functions at the Gaussian points can be done in $\mathcal{O}(p^3)$ operations. This is optimal in the three-dimensional case, but not in the two-dimensional case.

C.3 Complexity of the Algorithm

The cost of the last three steps in $\mathcal{O}(p^3)$, the first step requires $\mathcal{O}(p^2)$ operations. Together with the evaluation of the Jacobi polynomials, the algorithm requires in total $\mathcal{O}(p^3)$ flops.
This algorithm uses only the sparsity structure (C.3). Since the matrices A_s and M_s have a similar sparsity structure of the form (C.3), cf. Lemma 4.6, this algorithm can be extended to all ingredients which are required for the generation of A_s and M_s. For two-dimensional problems, the third step of the algorithm is not necessary. However, the values $h^{(2)}_{i,j;i',j'}$ have to be computed. Since this requires $\mathcal{O}(p^3)$ floating point operations, the total cost in 2D is also $\mathcal{O}(p^3)$.

D Sparsity relations for Legendre type basis functions

The auxiliary functions for the definition of cell based basis functions of Legendre-type are

$$\begin{aligned} u_i^L(x,y,z) &:= \hat{p}_i^0\left(\frac{\lambda_2-\lambda_1}{\lambda_2+\lambda_1}\right)(\lambda_2+\lambda_1)^i, \\ v_j^L(x,y,z) &:= \lambda_3 p_{j-1}^0\left(\frac{2\lambda_3-(1-\lambda_4)}{1-\lambda_4}\right)(1-\lambda_4)^{j-1}, \\ \text{and} \quad w_k^L(x,y,z) &:= \lambda_4 p_{k-1}^0(2\lambda_4-1), \end{aligned} \tag{D.1}$$

respectively. The cell-based basis functions are constructed following (4.5) and (4.6) and we denote the corresponding Legendre-type basis functions by $\chi_{ijk}^{(r)}$ and $\widetilde{\chi}_{ijk}^{(r)}$, $r=a,b,c$, respectively. Also for these basis functions a certain sparsity pattern can be observed, which occurs because of the Legendre orthogonality.
For the non-divergence free basis functions we note that

1. if $|k-n|>4$ then $\left(\nabla\cdot\widetilde{\chi}_{10k}^{(a)}, \nabla\cdot\widetilde{\chi}_{10n}^{(a)}\right)_{0,\hat{\triangle}} = 0$,
2. if $|j-m|>3$ then $\left(\nabla\cdot\widetilde{\chi}_{1jk}^{(b)}, \nabla\cdot\widetilde{\chi}_{1mn}^{(b)}\right)_{0,\hat{\triangle}} = 0$,

3. and if $i \neq l$ then $\left(\nabla \cdot \widetilde{\chi}^{(c)}_{ijk}, \nabla \cdot \widetilde{\chi}^{(c)}_{lmn}\right)_{0,\hat{\triangle}} = 0$.

The integrals in the remaining open parameters can be reduced to the following general type of integrals

$$\int_{-1}^{1} (1-z)^{\alpha} p^0_k(z) p^0_n(z)\, \mathrm{d}z, \quad \alpha = \alpha(i,j) \in \mathbb{N}.$$

By the Legendre orthogonality these integrals only vanish if either $i - j > \alpha$ or $-\alpha > i - j$. This yields the wedge-type shape of the sparsity pattern, but it results in an increasing number of nonzero entries with increasing polynomial degree. The situation for the mass matrix is, of course, similar but worse, i.e.,

1. if $|j-m| > 5$ then $\left(\chi^{(a)}_{1jk}, \chi^{(a)}_{1mn}\right)_{0,\hat{\triangle}} = 0$,
2. if $i \neq l$ then $\left(\chi^{(b)}_{ijk}, \chi^{(b)}_{lmn}\right)_{0,\hat{\triangle}} = 0$,
3. if $|i-l| \notin \{0,2\}$ then $\left(\chi^{(c)}_{ijk}, \chi^{(c)}_{lmn}\right)_{0,\hat{\triangle}} = 0$,
4. if $|k-n| > 6$ then $\left(\widetilde{\chi}^{(a)}_{10k}, \widetilde{\chi}^{(a)}_{10n}\right)_{0,\hat{\triangle}} = 0$,
5. if $j \neq m$ then $\left(\widetilde{\chi}^{(b)}_{1jk}, \widetilde{\chi}^{(b)}_{1mn}\right)_{0,\hat{\triangle}} = 0$,
6. and if $i \neq l$ then $\left(\widetilde{\chi}^{(c)}_{ijk}, \widetilde{\chi}^{(c)}_{lmn}\right)_{0,\hat{\triangle}} = 0$.

Acknowledgement: This work has been supported by the the Austrian Science Foundation (FWF) through grants P20121-N12, P20162-N18, and SFB/F32, the Austrian Academy of Sciences and the doctoral program "Computational Mathematics" (W1214).

References

[1] M. Abramowitz and I. Stegun, editors. *Handbook of mathematical functions.* Dover-Publications, 1965.

[2] M. Ainsworth and J. Coyle. Hierarchic finite element bases on unstructured tetrahedral meshes. *Int. J. Num. Meth. Eng.*, 58(14):2103–2130, 2003.

[3] G. E. Andrews, R. Askey, and R. Roy. *Special functions.* Number 71 in Encyclopedia of Mathematics and its applications. Cambridge University Press, 1999.

[4] D. N. Arnold, R. S. Falk, and R. Winther. Multigrid in $H(\mathrm{div})$ and $H(\mathrm{curl})$. *Numer. Math.*, 85(2):197–217, 2000.

[5] D. N. Arnold, R. S. Falk, and R. Winther. Differential complexes and stability of finite element methods I: The de Rham complex. In D. Arnold, P. Bochev, R. Lehoucq, R. Nicolaides, and M. Shaskov, editors, *Compatible Spatial Discretizations*, volume 142 of *The IMA Volumes in Mathematics and its Applications*, pages 23–46. Springer, Berlin, 2006.

[6] I. Babuška and M. Suri. The *p*- and *h-p* versions of the finite element method, an overview. *Comput. Methods Appl. Mech. Engrg.*, 80(1-3):5–26, 1990. Spectral and high order methods for partial differential equations (Como, 1989).

[7] A. Bećirović, P. Paule, V. Pillwein, A. Riese, C. Schneider, and J. Schöberl. Hypergeometric summation algorithms for high-order finite elements. *Computing*, 78(3):235–249, 2006.

[8] S. Beuchler and V. Pillwein. Shape functions for tetrahedral *p*-fem using integrated Jacobi polynomials. *Computing*, 80:345–375, 2007.

[9] S. Beuchler and V. Pillwein. Completions to sparse shape functions for triangular and tetrahedral p-fem. In U. Langer, M. Discacciati, D.E. Keyes, O.B. Widlund, and W. Zulehner, editors, *Domain Decomposition Methods in Science and Engineering XVII*, volume 60 of *Lecture Notes in Computational Science and Engineering*, pages 435–442, Heidelberg, 2008. Springer. Proceedings of the 17th International Conference on Domain Decomposition Methods held at St. Wolfgang / Strobl, Austria, July 3–7, 2006.

[10] S. Beuchler and J. Schöberl. New shape functions for triangular p-fem using integrated jacobi polynomials. *Numer. Math.*, 103:339–366, 2006.

[11] A. Bossavit. *Computational Electromagnetism: Variational formulation, complementary, edge elements*. Academic Press Series in Electromagnetism. Academic Press Inc., 1989.

[12] F. Brezzi and M. Fortin. *Mixed and hybrid finite element methods*. Springer-Verlag, Berlin, 1991.

[13] L. Demkowicz. *Computing with hp Finite Elements*. CRC Press, Taylor and Francis, 2006.

[14] L. Demkowicz and A. Buffa. h^1, h(curl) and h(div)-conforming projection-based interpolation in three dimensions. quasi-optimal p-interpolation estimates. *Computer Methods in Applied Mechanics and Engineering*, 194:267–296, 2005.

[15] L. Demkowicz, J. Kurtz, D. Pardo, M. Paszyński, W. Rachowicz, and A. Zdunek. *Computing with hp-adaptive finite elements. Vol. 2*. Chapman & Hall/CRC Applied Mathematics and Nonlinear Science Series. Chapman & Hall/CRC, Boca Raton, FL, 2008. Frontiers: three dimensional elliptic and Maxwell problems with applications.

[16] L. Demkowicz, P. Monk, L. Vardapetyan, and W. Rachowicz. De Rham diagram for hp finite element spaces. *Computers and Mathematics with Aplications*, 39(7-8):29–38, 2000.

[17] M. Dubiner. Spectral methods on triangles and other domains. *J. Sci. Computing*, 6:345, 1991.

[18] V. Girault and P.-A. Raviart. *Finite element methods for Navier-Stokes equations*, volume 5 of *Springer Series in Computational Mathematics*. Springer-Verlag, Berlin, 1986. Theory and algorithms.

[19] R. Hiptmair. Multigrid method for Maxwell's equations. *SIAM J. Numer. Anal.*, 36(1):204–225 (electronic), 1999.

[20] G.M. Karniadakis and S.J.Sherwin. *Spectral/HP Element Methods for CFD*. Oxford University Press. Oxford, 1999.

[21] T. Koornwinder. Two-variable analogues of the classical orthogonal polynomials. In *Theory and application of special functions (Proc. Advanced Sem., Math. Res. Center, Univ. Wisconsin, Madison, Wis., 1975)*, pages 435–495. Math. Res. Center, Univ. Wisconsin, Publ. No. 35. Academic Press, New York, 1975.

[22] J.M. Melenk, K. Gerdes, and C. Schwab. Fully discrete hp-finite elements: Fast quadrature. *Comp. Meth. Appl. Mech. Eng.*, 190:4339–4364, 1999.

[23] J.C. Nédélec. Mixed finite elements in $\mathbb{R}^3$. *Numerische Mathematik*, 35(35):315–341, 1980.

[24] J.C. Nédélec. A new family of mixed finite elements in $\mathbb{R}^3$. *Numerische Mathematik*, 50(35):57–81, 1986.

[25] S. A. Orszag. Spectral methods for problems in complex geometries. *J. Comp. Phys.*, pages 37–80, 1980.

[26] P. Paule, V. Pillwein, C. Schneider, and J. Schöberl. Hypergeometric Summation Techniques for High Order Finite Elements. In *PAMM*, volume 6, pages 689–690, Weinheim, 2006. Wiley InterScience. DOI: 10.1002/pamm.200610325.

[27] P.A. Raviart and J.M Thoma. A mixed finite element method for 2nd order elliptic problems. In *Mathematical aspects of finite element methods*, volume 606 of *Lecture Notes in Mathematics*. Berlin, 1977.

[28] J. Schöberl and S. Zaglmayr. High order Nédélec elements with local complete sequence properties. *COMPEL*, 24(2), 2005.

[29] C. Schwab. *p− and hp−finite element methods. Theory and applications in solid and fluid mechanics.* Clarendon Press. Oxford, 1998.

[30] S. J. Sherwin. Hierarchical *hp* finite elements in hybrid domains. *Finite Elements in Analysis and Design*, 27:109–119, 1997.

[31] S. J. Sherwin and G. E. Karniadakis. A new triangular and tetrahedral basis for high-order finite element methods. *Int. J. Num. Meth. Eng.*, 38:3775–3802, 1995.

[32] P. Solin, K. Segeth, and I. Dolezel. *Higher-Order Finite Element Methods.* Chapman and Hall, CRC Press, 2003.

[33] B. Szabo, A. Duester, and E. Rank. The p-version of the finite element method. In E. Stein, R. de Borst, and T. J. Hughes, editors, *Encyclopedia of Computational Mechanics.* Wiley, 2004.

[34] F.G. Tricomi. *Vorlesungen über Orthogonalreihen.* Springer. Berlin-Göttingen-Heidelberg, 1955.

[35] S. Zaglmayr. *High Order Finite Elements for Electromagnetic Field Computation.* PhD thesis, Johannes Kepler University, Linz, Austria, 2006.

Erschienene Preprints ab Nummer 2008/01

2008/1 P. Urthaler: Schnelle Auswertung von Volumenpotentialen in der Randelementmethode.

2008/2 O. Steinbach (ed.): Workshop on Numerical Simulation of the Maxwell Equations. Book of Abstracts.

2008/3 G. Of, O. Steinbach, P. Urthaler: Fast Evaluation of Newton Potentials in the Boundary Element Method.

2008/4 U. Langer, O. Steinbach, W. L. Wendland (eds.): 6th Workshop on Fast Boundary Element Methods in Industrial Applications, Book of Abstracts.

2008/5 D. Brunner, G. Of, M. Junge, O. Steinbach, L. Gaul: A Fast BE-FE Coupling Scheme for Partly Immersed Bodies

2009/3 G. Of, O. Steinbach: The All–Floating Boundary Element Tearing and Interconnecting Method.

2009/4 O. Steinbach: A note on the stable coupling of finite and boundary elements.

2009/5 O. Steinbach, M. Windisch: Stable boundary element domain decomposition methods for the Helmholtz equation.

2009/6 G. Of, W. L. Wendland, N. Zorii: On the Numerical Solution of Minimal Energy Problems.

2009/7 U. Langer, O. Steinbach, W. L. Wendland (eds.): 7th Workshop on Fast Boundary Element Methods in Industrial Applications, Book of Abstracts.

2009/8 H. Egger, M. Freiberger, M. Schlottbom: Analysis of Forward and Inverse Models in Fluorescence Optical Tomography.

2009/9 O. Steinbach, M. Windisch: Robust boundary element domain decomposition solvers in acoustics.

2009/10 M. Freiberger, H. Egger, H. Scharfetter: Nonlinear Inversion in Fluorescence Optical Tomography.

2009/11 H. Egger, M. Hanke, C. Schneider, J. Schöberl, S. Zaglmayr: Adjoint Sampling Methods for Electromagnetic Scattering.

2009/12 H. Egger, M.Schlottbom: Analysis and Regularization of Problems in Diffuse Optical Tomography.

2009/13 G. Of, T. X. Phan, O. Steinbach: An energy space finite element approach for elliptic Dirichlet boundary control problems.

2009/14 G. Of, O. Steinbach: Coupled FE/BE Formulations for the Fluid–Structure Interaction.

2010/1 G. Of, T. X. Phan, O. Steinbach: Boundary element methods for Dirichlet boundary control problems.

2010/2 P. D. Ledger, S. Zaglmayr: hp–Finite element simulation of three–dimensional eddy current problems on multiply connected domains.

2010/3 O. Steinbach, P. Urthaler: On the unique solvability of boundary integral equations in poroelasticity.

2010/4 S. Engleder, O. Steinbach: Boundary integral formulations for the forward problem in magnetic induction tomography.

2010/5 Z. Andjelic, G. Of, O. Steinbach, P. Urthaler: Direct and indirect boundary element methods for magnetostatic field problems.

2010/6 M. Neumüller, O. Steinbach: A space–time discontinuous Galerkin method for parabolic initial boundary value problems

2010/7 L. Tchoualag, G. Of, O. Steinbach: Circulant matrix methods for Yukawa type linear elasticity problems.

2010/8 A. Klawonn, U. Langer, L. F. Pavarino, O. Steinbach, O. B. Widlund (eds.): Workshop on Domain Decomposition Solvers for Heterogeneous Field Problems, Book of Abstracts.

2010/9 O. Steinbach, G. Unger: Convergence analysis of a Galerkin boundary element method for the Dirichlet Laplacian eigenvalue problem.

2010/10 O. Steinbach (ed.): Workshop on Computational Electromagnetics, Book of Abstracts